

Prediction of Scour Depth in Gravel Bed Rivers using Radio Frequency IDs: Application to the Skagit River

WA-RD 821.1

A.N. Papanicolaou
Iordanis Moustakidis
Achilleas Tsakiris
Christopher Wilson
Benjamin Abban

October 2013



**PREDICTION OF SCOUR DEPTH IN GRAVEL BED RIVERS
USING RADIO FREQUENCY IDs: APPLICATION TO THE SKAGIT
RIVER**

FINAL REPORT



Submitted to:
Washington State Department of Transportation, Research Program
Washington State Highway Research Board
310 Maple Park Ave SE
Olympia, WA 98504-7329

Submitted by:
Dr. Thanos Papanicolaou
IIHR-Hydrosience & Engineering
College of Engineering
The University of Iowa
Iowa City, Iowa 52242
October 2013

About the IIHR- Hydroscience & Engineering

IIHR, a unit of The University of Iowa's College of Engineering, is one of the nation's premier and oldest fluids research and engineering laboratories. Situated on the Iowa River in Iowa City, Iowa, IIHR seeks to educate students and to conduct research in the broad fields of hydraulics and fluid mechanics.

Disclaimer Notice

The contents of this report reflect the views of the author(s), who is (are) responsible for the facts and the accuracy of the data presented herein. The contents do not necessarily reflect the official views or policies of the Washington State Department of Transportation [and/or another agency]. This report does not constitute a standard, specification, or regulation.

The sponsors do not endorse products or manufacturers. Trademarks or manufacturers' names appear in this report only because they are considered essential to the objective of the document.

The opinions, findings, and conclusions expressed in this publication are those of the author and not necessarily those of the Washington State Department of Transportation.

Non-discrimination Statement

The University of Iowa does not discriminate on the basis of race, color, age, religion, national origin, sexual orientation, gender identity, sex, marital status, disability, or status as a U.S. veteran. Inquiries can be directed to the Director of Equal Opportunity and Diversity at the University of Iowa, (319) 335-0705.

Technical Report Documentation Page

1. REPORT NO. WA-RD 821.1		2. GOVERNMENT ACCESSION NO.		3. RECIPIENT'S CATALOG NO.	
4. TITLE AND SUBTITLE Prediction of Scour Depth in Gravel Bed Rivers using Radio Frequency IDs: Application to the Skagit River				5. REPORT DATE October 31st, 2013	
				6. PERFORMING ORGANIZATION CODE	
7. AUTHOR(S) Prof. A.N. (Thanos) Papanicolaou, Jordanis V. Moustakidis, Achilleas G. Tsakiris, Dr. Christopher G. Wilson & Benjamin Abban				8. PERFORMING ORGANIZATION REPORT NO.	
9. PERFORMING ORGANIZATION NAME AND ADDRESS IIHR- Hydroscience & Engineering The University of Iowa 300 South Riverside Drive Iowa City, Iowa 52242-1585				10. WORK UNIT NO.	
				11. CONTRACT OR GRANT NO. 18057000	
12. SPONSORING AGENCY NAME AND ADDRESS Washington State Highway Research Board Washington State Department of Transportation 310 Maple Park Ave Olympia, WA 98504-7329				13. TYPE OF REPORT AND PERIOD COVERED Final Report	
				14. SPONSORING AGENCY CODE	
15. SUPPLEMENTARY NOTES					
16. ABSTRACT The overarching goal of the proposed research was to develop, test and verify a robust system based on the Low Frequency (134.2 kHz), passive Radio Frequency Identification (RFID) technology to be ultimately used for determining the maximum scour depths near the proposed flow deflection structures located at MP 100.7 on the Skagit River. For the purposes of this study, a RFID system was assembled and utilized for developing calibration curves that relate signal voltage or equivalently RSSI (Received Signal Strength Indicator) with distance via detailed experiments for a range of stream bed conditions (i.e., gravel- and sand-size bed material) in laboratory and quarry environments.					
17. KEY WORDS Key words: Gravel bed river, RFID, maximum scour depth, RSSI, deflection structures			18. DISTRIBUTION STATEMENT No restrictions.		
19. SECURITY CLASSIF. (of this report) None		20. SECURITY CLASSIF. (of this page) None		21. NO. OF PAGES	22. PRICE NA

Reproduction of completed page authorized

**PREDICTION OF SCOUR DEPTH IN GRAVEL BED RIVERS
USING RADIO FREQUENCY IDS: APPLICATION TO THE SKAGIT
RIVER**

**Final report
October 2013**

Principal Investigator
Dr. Thanos Papanicolaou
Professor
IIHR - Hydroscience & Engineering
The University of Iowa
Iowa City, IA 52242

Sponsored by
the Washington State Highway Research Board

A report from
IIHR-Hydroscience & Engineering
College of Engineering
The University of Iowa
Iowa City, Iowa 52242
Phone: 319 335-5237
Fax: 319 335 5238
www.iihr.uiowa.edu

ACKNOWLEDGEMENTS

This study was funded by the WSDOT research program led by Rhonda Brooks.

The writers are indebted to Casey Kramer, Project Director, Hydraulic Engineer, WSDOT for all the help that he provided during the project. The writers would like also to thank Will Ettema, Dr. Filippo Bressan for their help with the completion of the field work.

The interaction with Oregon's RFID Warren Leach has been very informative and constructive.

TABLE OF CONTENTS

	<u>Page</u>
ACKNOWLEDGEMENTS	v
TABLE OF CONTENTS	vi
1. INTRODUCTION	1
1.1 Problem statement and background	
1.2 Objectives and Tasks	
1.3 Methodology	
1.3.1 TI RFID system configuration	
1.3.2 Experimental design and setup	
1.3.2.1 Laboratory experimental setup	
1.3.2.1.1 Transponder housing experiments	
1.3.2.1.2 Transponder orientation effects on the transponder return RF signal (RSSI)	
1.3.2.1.3 Medium effects on the RF signal strength decay (RSSI)	
1.3.2.1.4 Location of the buried transponder in the 3-D domain	
1.3.2.2 Field experimental setup	
1.3.2.2.1 Development of a custom made excitation antenna	
1.3.2.2.2 RF signal strength calibration curves developed in the field	
1.4 Transponder's return RF signal strength analysis (RSSI)	
2. RESULTS	24
2.1 Laboratory results	
2.1.1 Transponder housing experiments	
2.1.2 Transponder orientation effects on the transponder return RF signal	
2.1.3 Medium effects on the RF signal strength decay (RSSI)	
2.1.4 Location of the buried transponder in the 3-D domain	
2.2 Field results	
2.2.1 RF signal strength calibration curves developed in the field	
2.2.1.1 Flow point measurements	
2.2.1.2 Remote flow measurements via LSPIV	
2.2.1.3 Stage-Discharge equations	
2.2.2 Turbulent flow characteristics	
2.2.3 Energy dissipation	
3. CONCLUSIONS AND SUMMARY	38
4. OUTCOMES AND RECOMMENDATIONS	39
5. REFERENCES	40

LIST OF FIGURES

	<u>Page</u>
Figure 1-1. TI RFID reader.	2
Figure 1-2. RFID excitation antennas. (A) TI RFID off-the-shelf excitation antenna (http://rfidusa.com/superstore/product_info.php?cPath=38_27&products_id=100); and (B) Custom made RFID excitation antenna constructed in the field to meet the specific project needs (http://www.oregonrfid.com/overview/index.html).	2
Figure 1-3. TI RFID transponders. (A) 23 mm glass encased penny size comparison; and (B) 120 mm long transponder.	3
Figure 1-4. Papanicolaou et al. 2010 scour experiments using the TI RFID system.	4
Figure 1-5. TI RFID system main components.	6
Figure 1-6. Information stored into the transponder internal memory (i.e., transponder serial number (S/N)).	7
Figure 1-7. Transponder detection software for the TI RFID system, developed in IIHR.	8
Figure 1-8. Size comparison for the transponder and particles used. from left to right: (A) “naked” transponder, (B) concrete-encased particle and (C) red painted rock-encased particles. The transponder density is 2,223Kg/m ³ .	9
Figure 1-9. Transponder’s main orientations with respect to the excitation antenna plan; (a) perpendicular and (b) parallel.	10
Figure 1-10. Schematic representation of the experimental setup for testing the medium effects on the transponder return RF signal; $D_{a-t,max}$ is the maximum detection distance achieved between the excitation antenna and the transponder.	11
Figure 1-11. Erosion process experimental setup.	12
Figure 1-12. Deposition process experimental setup.	12
Figure 1-13. Schematic representation of the applied triangulation method to locate the position of the buried transponder in the 2-D domain.	14
Figure 1-14. Triangulation experimental setup to identify three points located at the limits of the transponder’s electromagnetic field.	14
Figure 1-15. Schematic representation of the applied triangulation method to locate the position of the buried transponder in the 3-D domain, by raising the excitation antenna right above the plane location of the transponder.	15
Figure 1-16. (A) Custom excitation antenna’s performance evaluation setup and (B) PVC encased transponder developed by TI.	18
Figure 1-17. Willow Creek Park experimental setup for developing RF signal strength calibration curves in air.	19
Figure 1-18. Willow Creek Park experimental setup for developing RF signal strength calibration curves in sand and gravel mediums. (a) Side view of the experimental setup with the wooden structure and the PVC pipes on top of it and the custom made excitation antenna and (b) Filling the PVC pipes with material to bury the transponder.	20
Figure 1-19. Quarry RFID experimental setup. A 18 ft. deep hole was drilled to place the transponder.	20
Figure 1-20. RFID transponders’ installation location in Clear Creek near Camp Cardinal in Johnson County, IA (location coordinates: 41°40’35” N and 91°35’55” W).	21
Figure 1-21. Transponder stream bed installation process setup.	21
Figure 1-22. Field monitoring setup to obtain the RF signal strength of each transponder.	22

Figure 1-23. One RF signal cycle (~ 0.1 seconds) main parts and time lengths.	23
Figure 1-24. Development of RFID reader voltage vs. antenna-transponder distance calibration curves.	23
Figure 2-1. Antenna-transponder maximum detection distances for different transponder housing material (i.e., “naked”, “rock”- and “concrete”- encasement) after a total of 16 iterations.	24
Figure 2-2. Medium and orientation effects (i.e., $\phi = 90, 0, 60$ and 30° transponder long axis orientation with respect to the excitation antenna plane) on the transponder return RF signal strength (RSSI) in air.	27
Figure 2-3. Transponder detection success percentage rate as a function of the antenna-transponder distance, for each transponder used in this experimental series.	28
Figure 2-4. RF signal strength decay curves developed in different mediums in between the excitation antenna and the transponder (i.e., air, water, sand and gravel) for the favorable transponder orientation (i.e., $\phi = 90^\circ$ with respect to the excitation antenna plane).	29
Figure 2-5. Medium and orientation effects (i.e., $\phi = 90, 0, 60$ and 30° transponder long axis orientation with respect to the excitation antenna plane) on the transponder return RF signal strength (RSSI) in water.	30
Figure 2-6. Medium and orientation effects (i.e., $\phi = 90, 0, 60$ and 30° transponder long axis orientation with respect to the excitation antenna plane) on the transponder return RF signal strength (RSSI) in sand.	31
Figure 2-7. Medium and orientation effects (i.e., $\phi = 90, 0, 60$ and 30° transponder long axis orientation with respect to the excitation antenna plane) on the transponder return RF signal strength (RSSI) in gravel.	32
Figure 2-8. Screenshot of the triangulation code, requiring the user to insert the 3 antennas GPS coordinates to calculate the location of the buried transponder in the x-y plane (2D domain).	34
Figure 2-9. Transponder return RF signal strength decay curves in various mediums (i.e., air, water, sand and gravel) using the custom made excitation antenna developed by Papanicolaou research group.	36
Figure 2-10. Processed RF signal strength decay curves corresponding to the two measurement dates during this reporting period: 04/05/2013 and 06/07/2013.	37

LIST OF TABLES

Table 1-1. Summary of the “laboratory” experiments performed.	8
Table 1-2. Effects of transponder housing material on the maximum detection distance.	9
Table 1-3. Summary of the “field” experiments performed.	15
Table 2-1. Components of the proposed RFID system.	25

1. INTRODUCTION

1.1 Problem statement and background

Scour has been identified as a problem of national scope, being both an economic burden and a threat to public safety (ASCE 2012). The term scour is used to define the removal of channel bed sediments under the erosive action of the flow. Excessive scour can dramatically affect channel stability by exposing the subsoil and laterally eroding the riverbanks (Ettema et al. 2006). This channel instability greatly increases the potential for failure of the hydraulic structures (i.e., piers, deflections, dikes, spurs, bank deflectors) located within the channel boundaries.

The current methods which have employed to quantify scour depths (i.e., sounding poles and sounding weights, also known as physical probes) cannot be effectively used during high flows, when the maximum scour occurs, since the safety of the inspection crew can be at risk (Fukui and Otuka 2002). The intrusive nature of the physical probes also tend to affect their accuracy by 60-80% under the action of violent hydrodynamic forces. Therefore, there is a critical need for an advanced system of a non-intrusive nature that can provide WSDOT engineers and inspection crews with reliable scour data under all circumstances.

There is a critical need for an advanced system of a non-intrusive nature that can provide WSDOT engineers and inspection crews with reliable scour data under all circumstances.

To address this critical need, as a first step, the Radio Frequency Identification (RFID) technology is adopted and enhanced here for improving the understanding of the scour process, especially, around 3-D bluff objects such as the Engineered Log Jams (ELJs) (NRCS, 2007; Stream Restoration Design of the National Engineering Handbook (NEH) Part 654 (Chapter 14)). RFID is a relatively new technology that utilizes Radio Frequency (RF) waves to transfer information between a base station (i.e., reader) and a sensor (i.e., transponder) via an excitation antenna (e.g., Finkenzeller 2010). The “non-line-of-sight” communication between the reader and a transponder is considered an important RFID feature based on which a non-intrusive, non-destructive scour monitoring system can be developed.

RFID is a relatively new technology that utilizes Radio Frequency (RF) waves to transfer information between a base station (i.e., reader) and a sensor (i.e., transponder) via an excitation antenna.

A typical RFID system consists of three main parts; namely, (i) the reader, which is a set of circuit boards that transmits RF signals through an excitation antenna to a transponder (Figure 1-1), (ii) the excitation antenna, which ensures the two-way communication between the reader and a transponder through electronic circuits (i.e., antenna tuning board) (Figure 1-2), and (iii) the transponders (short for transmitter/responder) that sends out a coded ID, as well as other stored data, to the reader

(Figure 1-3). The excitation antenna relays this information (i.e., transponder ID and stored data) to the reader, which passes them to a host device, or a computer. The RFID transponders can be classified either as passive, where the reader wakes up the transponder via the excitation antenna's magnetic field, or active, where the power source (i.e., battery) is embodied into the transponder, or semi-passive, where the transponder is activated by the reader, while it uses its power source to transmit the data back to the reader (Roberts 2006). An oscilloscope is used to capture the time series of the return signal.

Another key distinction between active and passive RFID systems is their operational frequency. Most of the active RFID systems operate in High Frequency (HF) band, while passive systems in Low Frequency (LF). The importance of the frequency band relates to the properties of the HF and LF waves, where the LF waves (i) can easily penetrate into saturated sediment and (ii) are less affected by the presence of metal structures compared to the HF waves (Personal communication with Telonics).

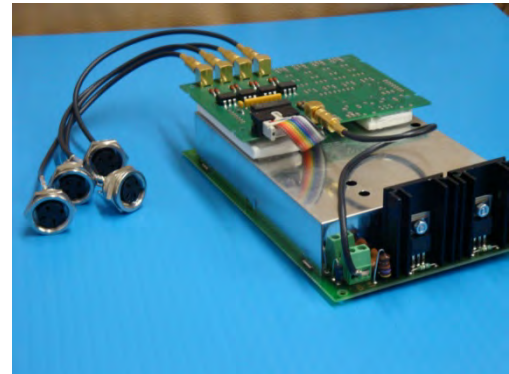


Figure 1-1. TI RFID reader.

One of the very first applications of the RFIDs was during WWII, where the British Royal Air Force supplied its aircrafts with transponders in order to efficiently recognize friendly from enemy planes (Dittmer 2004; Domdouzis 2007). During the 1970s, RFID technology really bloomed and became an integral part of many applications in different disciplines.

In the retail industry, products are assigned with RFID transponders to help the management of keeping track of these products and avoid their misplacement and theft (Roussos 2006; Gaukler et al. 2007; Rekik 2008; Sellito et al. 2007). In construction industry, where people's movement, tool and equipment location, as well as construction material control are of a primary concern, RFIDs have been successfully employed to meet these critical needs (Jaselskis et al. 1995; Goodrum et al. 2006; Wang et al. 2007; Ko 2010). RFIDs have also been extensively used in controlling and managing road traffic by tracking vehicles and regulating the traffic flow

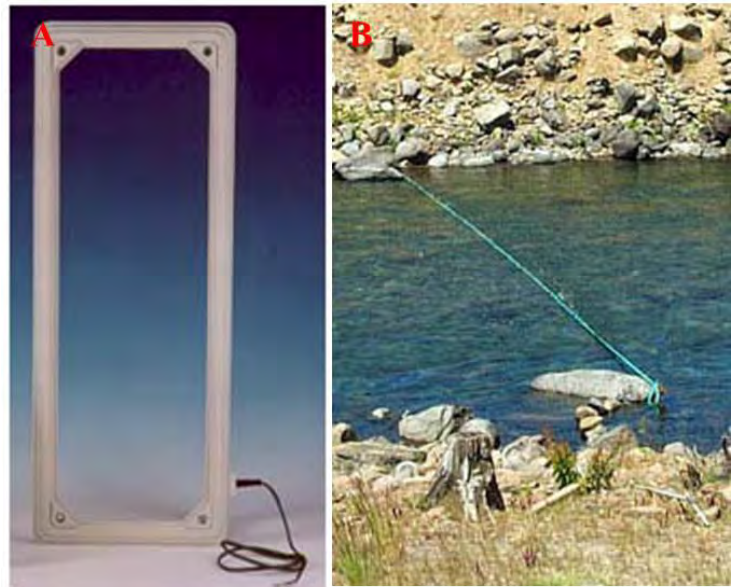


Figure 1-2. RFID excitation antennas. (A) TI RFID off-the-shelf excitation antenna (http://rfidusa.com/superstore/product_info.php?cPath=38_27&products_id=100); and (B) Custom made RFID excitation antenna constructed in the field to meet the specific project needs (<http://www.oregonrfid.com/overview/index.html>).

in order to solve congestion problems especially in metropolises (Wen 2008; Chattaraj et al. 2009; Wen 2010). However, active RFIDs have been employed in most of these studies due to the fact that active transponders have significantly longer reading range in air compared to passive ones. Several studies have used passive RFIDs for tracking objects in the 3-D domain.



Figure 1-3. TI RFID transponders. (A) 23 mm glass encased penny size comparison; and (B) 120 mm long transponder.

These studies have focused on the establishment of quantitative relations between the Received Signal Strength Indication (RSSI) and the distance of the transponder from the reader, as well as develop algorithms for locating tagged items in the 3-D domain (Zhao et al. 2006; Choi et al. 2009; Joho et al. 2009; Khan and Antiwal 2009; Ko 2010).

In scour monitoring, the RFID technology has not been extensively employed. In fact, only few attempts have been made to explore the potential advantages of the RFID technology in the scour monitoring field. In most of these studies, passive RFID transponders have been employed, since active transponders (i) are very expensive (~\$300/active transponder) and therefore a limited number of transponders can be acquired, (ii) have much bigger dimensions, due to the fact that the power source (i.e., battery) is embodied, which makes them difficult to handle during installation at the field, (iii) require periodic maintenance due to battery limited lifetime and (iv) due to the dilution of the RF signal triggered from the significant backscatter when the HF waves travel through water or sediment (Choritos 1998; Personnal communication with Telonics).

Papanicolaou et al. (2010) pioneered the use of a LF, passive RFID system to monitor scour around a model hydraulic structure (i.e., bridge piers). In this study, glass encased transponders, named scour balls, were buried at various depths in the vicinity of a bridge pier, where the maximum scour was expected (Figure 1-4). Each transponder was programmed with a unique ID and data regarding its initial burial depth and position with reference to the bridge pier were recorded. As the scour progressed and reached the burial depth of a scour ball, the scour ball



Figure 1-4. Papanicolaou et al. 2010 scour experiments using the TI RFID system.

transponder (iii) developing RF signal strength decay curves in various mediums (i.e., air, water, sand and gravel) and (iv) assigning an ID number for each tag (see Fig.). In an unpublished proposal study by Chen et al. (2011) was stated that passive and ultrasonic active RF sensors would be employed to monitor scour around a hydraulic structure (i.e., bridge pier). They intend to install the RF sensors into rocks (smart rocks) and bury them around a bridge pier. As scour progresses, the smart rocks or rocks tagged with RFIDs will be exposed and gathered into the scour hole formed. The RF sensors will transmit critical spatial and temporal information about the scour evolution at all times. Ultrasonic active transponders have been successfully used in sediment transport studies in gravel bed rivers, where the flow depth in some cases was 12 m (Habersack 2001; Liedermann 2012). Finally, in a laboratory study conducted by Hawrylak and Mickle (2009), HF active RFID transponders (433 MHz) were employed by the bridge inspection personnel to provide visual assessments about the bridge scour evolution. However, the system's performance has not been yet tested and validated in real field conditions.

Based on these promising findings, the authors believe that the LF, passive RFID technology warrant the potential to be effectively used as an advanced scour monitoring system. However, two major limitations emerged through the literature review; namely, (i) the short reading distances of the LF, passive RFID systems, which varies from few centimeters to a meter and (ii) the fact that no systematic field experiments have been performed.

1.2 Objectives & Tasks

The overarching objective of this project is to develop the technology for permitting the determination of the maximum scour depths near proposed flow deflection structures such as ELJs to be installed at MP 100.7 on the Skagit River using the IIHR Radio Frequency

Identification (RFID) system. The corresponding tasks of this study can be summarized as follows:

- A. Calibration curves that relate voltage with distance for different water depths/gravel depth combinations.
- B. Design of a field RFID system, including specifically the antenna, cable, power options, and a datalogger.
- C. Relation of a Global Position System (GPS) location for the RFID reader system to the transponders.
- D. Comparison with other options (i.e., alternative methods, such as sonar) to verify the RFID readings before and after an event.
- E. A report outlining the steps of how to build an RFID system and how to operate it.

1.3 Methodology

1.3.1 TI RFID system configuration

For the purposes of this study, a Low Frequency (LF) (134.2 kHz), passive RFID system developed by Texas Instruments (TI) was employed (Figure 1-5). This RFID system consists of three main parts. The first part is the reader, which is a set of two boards, namely the control and the radio frequency modules. The frequency module converts the RF waves transmitted by the transponder into electrical signals that can be then processed by the control module and send to the host computer. The control module is the interface between the frequency module and the PC, which is used to control the system (Papanicolaou et al 2010). Essentially, the control module converts the RF signals received from the transponder into the serial number (ID) of the transponder and transmits this information over a serial line to the host PC. The type of reader used in this study, is considered as the most powerful and durable offered by TI and thus, the RF signal emitted by the reader is very strong, which considerably increases the maximum detection distance between the excitation antenna and the transponder (Personal communication with TI engineers).

The excitation antenna is the second component and also consists of circuits (e.g., antenna tuning module) that ensure the two-way communication between the reader and the transponder. Two excitation antennas were used in this study, (1) an off-the-shelf TI large rectangular loop shape antenna with dimensions of $0.70 \times 0.70 \text{ m}^2$ and (2) a custom made square loop shape antenna with dimensions of $3 \times 1.83 \text{ m}^2$. The two excitation antennas can be interchangeably connected to the reader by switching two pin

Another advantage that the TI RFID system offers is that a custom made excitation antenna can be connected to the reader. This option allows the user to build an optimal antenna by manipulating the size, material and shape of the antenna to increase the maximum detection distance.

type connectors.

Another advantage that the TI RFID system offers is that a custom made excitation antenna can be connected to the reader. This option allows the user to build an optimal antenna by manipulating the size, material and shape of the antenna to increase the maximum detection distance. A 10 m long waterproof twinax cable was used to connect the selected excitation antenna with the reader. The length of the twinax cable can be up to 120 m. For lengths more than 120 m, the resistance will increase resulting in reduced antenna voltage, directly affecting the maximum antenna-transponder detection distance (Oregon RFID 2012). The antenna tuning module (Large Tuner Board) tunes the excitation antenna with the reader to ensure that the outgoing RF signal emitted by the frequency module is at the correct frequency for proper communication between the reader and the transponder.

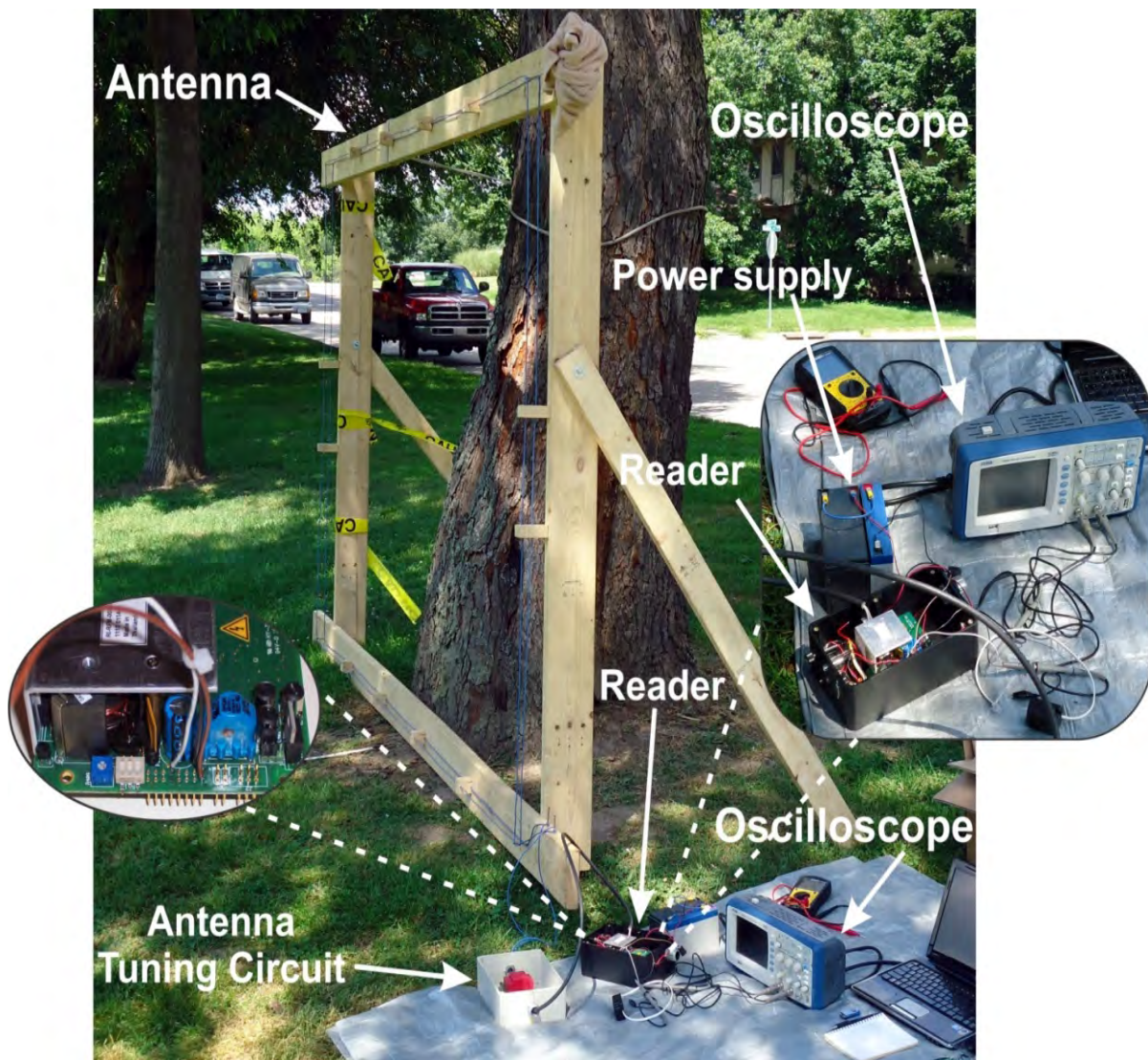


Figure 1-5. TI RFID system main components.

The passive transponders are the third component and embody circuits that allow the information sent by the reader to be stored and sent back as a response RF signal to the reader; a miniature antenna that supports the two-way communication between the reader and the transponder and capacitors to store the charge up energy transferred through the excitation antenna's electromagnetic field (Nichols 2004).

Two transponder types were selected for this study. The TI 23 mm long, cylindrical, low frequency, passive transponders and the TI 120 mm long, cylindrical, low frequency, passive transponders were used (shown earlier in Figure 1-3). The low acquisition cost of each transponder permitted the purchase of a large number of transponders of the two types. Each transponder came with 80 bit Read/Write memory, which enabled the assignment of a unique identification number (transponder ID) on each transponder shown in Figure 1-6. The ability to assign each transponder with a unique serial number was the basis for developing, in IIHR - Hydroscience & Engineering laboratory, a code in C++ language, which records the number and the detection time of each transponder and exports the output in a text file format (Figure 1-7). The entire TI RFID system is powered by two batteries of 12 and 6 Volt connected in series and resulting in 18 Volt power supply. The maximum RFID system allowed voltage is 20 Volts (TI Series 2000 Reader System Reference Guide, 2008).

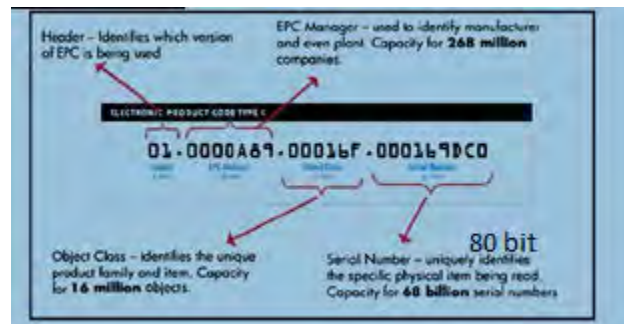


Figure 1-6. Information stored into the transponder internal memory (i.e., transponder serial number (S/N)).

The TI RFID system operates as half-duplex. In other words, one read cycle (lasts approximately 0.1 seconds) has two phases:

- Phase 1 (or “emitting” phase) where for the first 0.05 seconds the reader sends RF waves at the frequency of 134.2 kHz, to charge the transponder’s circuitry (transponder’s internal capacitors) and
- Phase 2 (or “listening” phase) where for the last 0.05 seconds the reader is receiving the RF signal from the transponder. Therefore, the half-duplex system ensures the regular and undisturbed communication between the reader and the transponder, since when the one is in the “emitting” mode; the other is in the “listening” mode.

Finally, a 25 MHz digital storage oscilloscope by B&K PRECISION (2530B) was connected to the RFID reader radio frequency board, to the J1 connector’s pins #1, 2, 6 and 10, which corresponded to logic ground, transmitter control input for activation of the transmitter (active low, internal pull-up resistor), logic level compatible receiver clock output and analog receiver signal strength test pin functions, respectively. The digital oscilloscope was used to record and export the shape and form of the RF signal.

1.3.2 Experimental design and setup

The performance of the TI RFID system was evaluated by conducting carefully designed laboratory and field experiments to determine the system reading range when various mediums (i.e., air, water, sand and gravel) are placed between the excitation antenna and the transponder, as well as to relate the transponder return RF signal strength (Received Signal Strength Indicator – RSSI) with the distance between the transponder and the excitation antenna, under various mediums and water depth / medium height combinations. Other important factors that can significantly affect the performance of an RFID system by deteriorating the reading range of the system and will be examined in this study are: (i) the housing effects (Lauth and Papanicolaou, 2009); (ii) the transponder orientation with respect the excitation antenna plane (Clarke et al., 2006); and (iii) the placement of the excitation antenna right on top of the transponder location (triangulation) (Dziadak et al. 2009). Laboratory experiments were first conducted in order to provide controlled conditions during the tests (Table 1-1), followed by field experiments to assess the applicability of the RFID technology in the field under different weather conditions (Table 1-3). The findings of these lab and field experiments will facilitate the development of an integrated system to monitor scour around hydraulic structures for phase II of the ongoing contract.

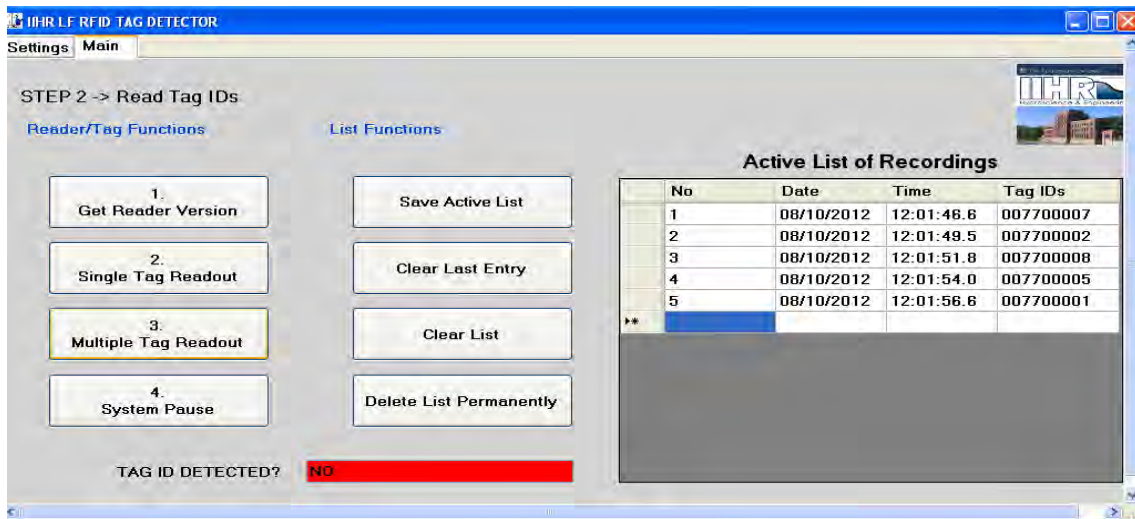


Figure 1-7. Transponder detection software for the TI RFID system, developed in IIHR.

1.3.2.1 Laboratory experimental setup

1.3.2.1.1 Transponder housing experiments

The effects of the transponder housing material on the reading range of the LF, passive RFID system developed by TI were examined herein (overall of 10 runs were performed). The TI 23 mm long cylindrical transponders were employed for these experiments, since it was easier to install them into rock- and concrete- particles (Figure 1-8). First, a “naked” transponder (no

housing material used) was tested to determine the maximum detection distance. The transponders were moving gradually away from the excitation antenna and the distance at which the communication between the excitation antenna and the transponder was lost was considered to be the maximum detection distance. The same procedure was followed for rock- and concrete- encased transponders (Table 1-2). As it was expected, the maximum detection distance occurred for the “naked” transponders, while the concrete-encased transponders had the poorest performance resulting in a 22.1% reduction of the maximum detection distance compared to the “naked” transponders. The rock-encased transponder though had an intermediate performance compared to the “naked” and concrete-encased transponders, resulting in a 10.3% reduction of the maximum detection distance.



Figure 1-8. Size comparison for the transponder and particles used. from left to right: (A) “naked” transponder, (B) concrete-encased particle and (C) red painted rock-encased particles. The transponder density is 2,223Kg/m³.

Housing material	“Naked”	Rock-encased	Concrete-encased
Detection distance (m)	0.68*	0.61*	0.53*

* Average of 10 iterations, the deviation was ± 2% in the reported average values.

Table 1-2. Effects of transponder housing material on the maximum detection distance.

1.3.2.1.2 Transponder orientation effects on the transponder return RF signal (RSSI)

A total of 15 experimental runs were conducted to isolate the effects of the transponder’s inner antenna and long axis orientation towards the excitation antenna plane. In all runs the transponder was considered “naked”, meaning that it was encased in only the factory packaging, a reinforced poly-ether-imide encasing. This was considered as the baseline condition. For the baseline condition, the maximum antenna-transponder detection distance was considered to be 0.6 m ($D_{a-t,max}$), as it was reported by the manufacturer (TI Low Frequency 23 mm Glass Transponder Manual 2001). The following equipment was used during these experiments: the TI

low frequency, passive RFID system, the rectangular loop shape antenna, a TI 23 mm long, cylindrical transponder and a 25 MHz digital storage oscilloscope.

During these experiments 4 different transponders were used, while the transponders' long axis was placed at different orientations with respect to the excitation antenna plane (i.e., 0, 30, 60 and 90°) and the largest detection distance was recorded (Figure 1-9) (Clarke et al., 2006). The antenna–transponder distance was increased until the transponder was no longer detected by the excitation antenna following the methodology of Clarke et al. (2006). For each tested detection distance, the excitation antenna was swept over the transponder 16 times providing a total number of 64 chances to detect the transponder. The next step was to identify the effects of the transponder inner antenna on the maximum detection distance, along with the transponder's long axis orientation with respect to the excitation antenna plane.

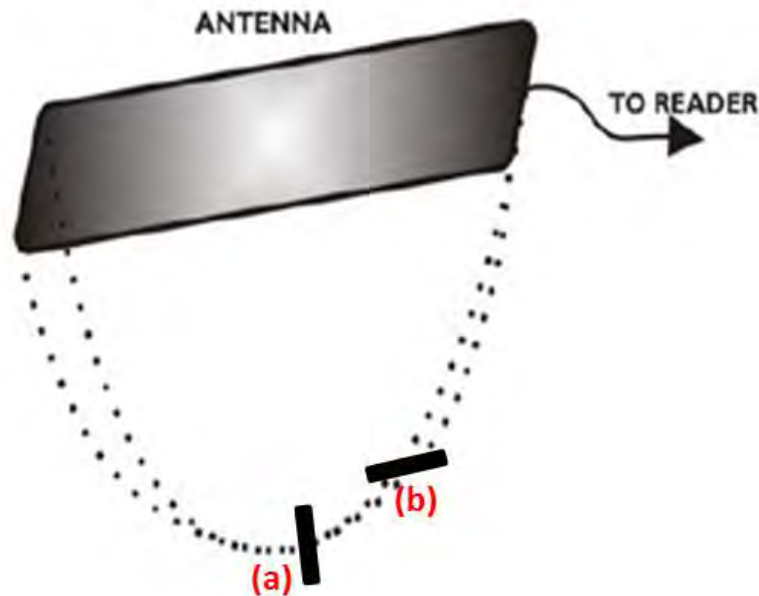


Figure 1-9. Transponder's main orientations with respect to the excitation antenna plan; (a) perpendicular and (b) parallel.

1.3.2.1.3 Medium effects on the RF signal strength decay (RSSI)

A number of 8 experimental runs were designed and performed to address the question of the effects of the medium type on the transponder return RF signal strength for the TI LF passive

RFID system with the TI 120 mm transponders. Each experimental run was repeated 5 times. Four different types of material, namely air, water, sand and gravel were considered and tested, for four transponder's long axis orientations, 0, 30, 60 and 90° with respect to the excitation antenna plane, respectively.

A plastic barrel with diameter and depth of 0.55 and 1.50 m respectively, resulting in a total volume of 0.356 m³ was employed to accommodate the experiments. The use of a plastic barrel to carry out the experiments was mainly sought because plastic does not affect the RF signal characteristics and the process of adding and removing material was simplified. The distance between the excitation antenna and the transponder for successfully detecting the latter was measured ($D_{a-t,max} = 1.50$ m) and recorded and the shape and the form of the transponder's return RF signal was analyzed at four measuring points corresponding to $D_{a-t,max}$, $3(D_{a-t,max})/2$, $D_{a-t,max} / 2$ and $D_{a-t,max} / 4$ of the detection distance, for each experimental case. The transponder return RF signal time series were recorded via a digital oscilloscope and then analyzed in MATLAB to estimate the RSSI value for each medium used. Figures 1-10, 1-11 and 1-12 show the experimental setup followed herein.

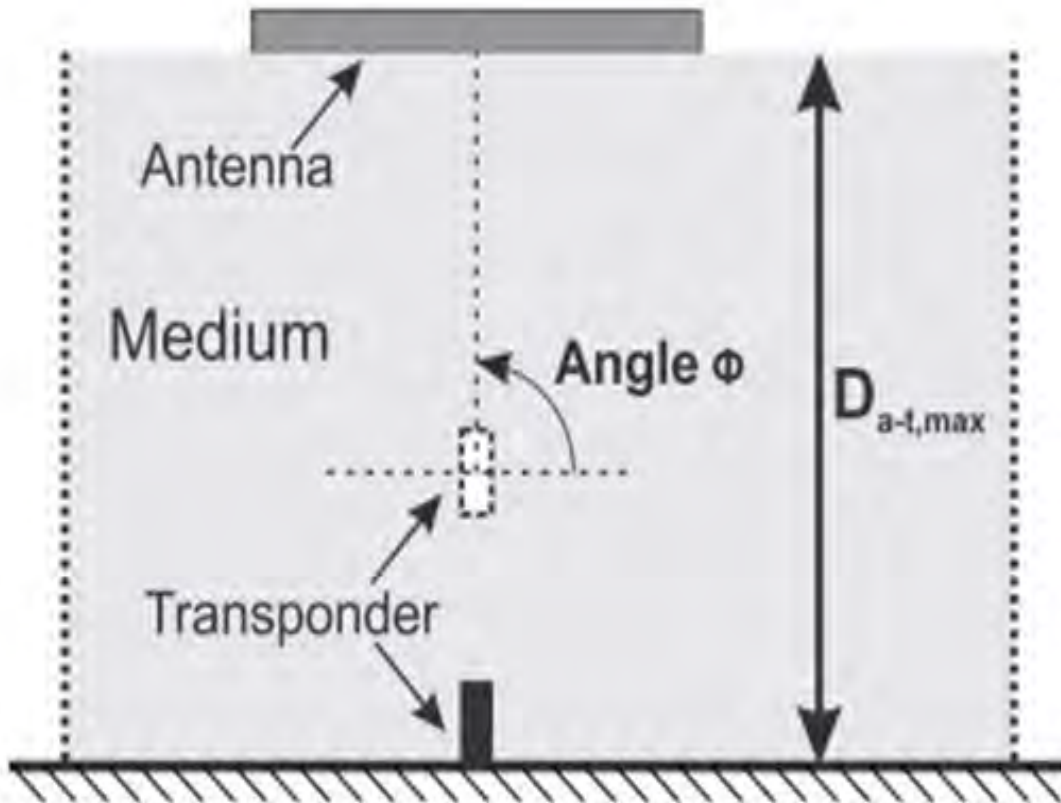


Figure 1-10. Schematic representation of the experimental setup for testing the medium effects on the transponder return RF signal; $D_{a-t,max}$ is the maximum detection distance achieved between the excitation antenna and the transponder.



Figure 1-11. Erosion process experimental setup.



Figure 1-12. Deposition process experimental setup.

1.3.2.1.4 Location of the buried transponder in the 3-D domain

A very important parameter related to the RF signal strength (RSSI) that can affect the performance of the TI LF passive RFID system is the placement of the excitation antenna right above the location of the buried transponder. The RFID reader provides the required energy to the excitation antenna and based on its technical characteristics (i.e., inductance, quality factor) the excitation antenna creates a “bulb” shaped electromagnetic field. The transponder inner antenna though is a unidirectional one, meaning that transmits only in one direction. Therefore, if the transponder is located closer to the limits of the excitation antenna electromagnetic field, the RSSI value would be much lower even though the exact antenna-transponder distance is quite small, leading to false conclusions about their actual distance.

The transponder orientation, the type of the material found in between the antenna and the transponder, as well as the transponder housing material are key-aspects of our experimental set-up.

To address this issue, a triangulation method will be employed to develop a code in C++ programming language, which will allow the user to find first the position of the buried transponder in the 2-D domain (i.e., x-y plane) by placing the excitation antenna at three points located at the limits of the electromagnetic field created by the transponder and record their coordinates using a Global Positioning System (GPS) device (Figure 1-13 and 1-14). The GPS coordinates of the three points will be fed to the triangulation algorithm, which will calculate the coordinates of the buried transponder in the 2-D domain. Once the location of the buried transponder has been successfully identified in the x-y plane, the user will place the excitation antenna right above the burial location of the transponder and the transponder return RSSI value will be recorded. Then, by comparing the RSSI value with the calibration curves that have been specifically developed for the type of medium in between the excitation antenna and the transponder, the transponder burial depth (transponder position in the 3-D domain) can be found (Figure 1-15). A total number of four experimental runs were conducted.

The triangulation method is based on the theory of circumcircle, which states that a polygon (i.e., triangle) can be circumscribed into a circle, where the perpendicular bisectors (radius r of the circle) meet in a single point known as the circumcenter (the center of the circumscribed circle) (Dziadak et al. 2009). The center of the circumscribed circle (which coincides with the location of the buried transponder in the 2-D domain) can be found using the following equations:

Circumscribed circle equation:

$$(x \pm x_t)^2 + (y \pm y_t)^2 = r^2 \quad (3-1)$$

Applying equation (3-1) for the antenna center points yields:

$$(x_1 - x_t)^2 + (y_1 - y_t)^2 = r^2 \quad (3-2)$$

Solving equations (3-2), (3-3) and (3-4) for the transponder location (x_t, y_t) yields:

$$(x_3 - x_t)^2 + (y_3 - y_t)^2 = r^2 \quad (3-4)$$

$$x_t = \frac{x_2^2 y_3 - x_2^2 y_1 - x_1^2 y_3 + y_2^2 y_3 - y_2^2 y_1 - y_1^2 y_3 - x_3^2 y_2 + x_3^2 y_1 + x_1^2 y_2 - y_3^2 y_2 + y_3^2 y_1 + y_1^2 y_2}{2 x_2 y_3 - 2 x_2 y_1 - 2 x_1 y_3 - 2 x_3 y_2 + 2 x_3 y_1 + 2 x_1 y_2} \quad (3-5)$$

$$y_t = \frac{x_2^2 - x_1^2 - 2 x_t (x_2 - x_1) + y_2^2 - y_1^2}{2(y_2 - y_1)} \quad (3-6)$$

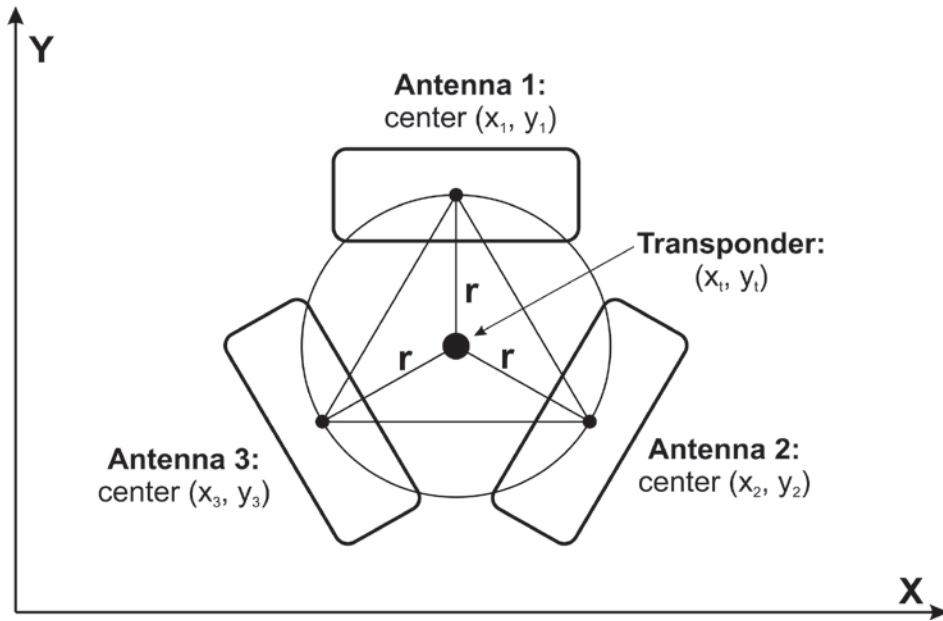


Figure 1-13. Schematic representation of the applied triangulation method to locate the position of the buried transponder in the 2-D domain.



Figure 1-14. Triangulation experimental setup to identify three points located at the limits of the transponder's electromagnetic field.

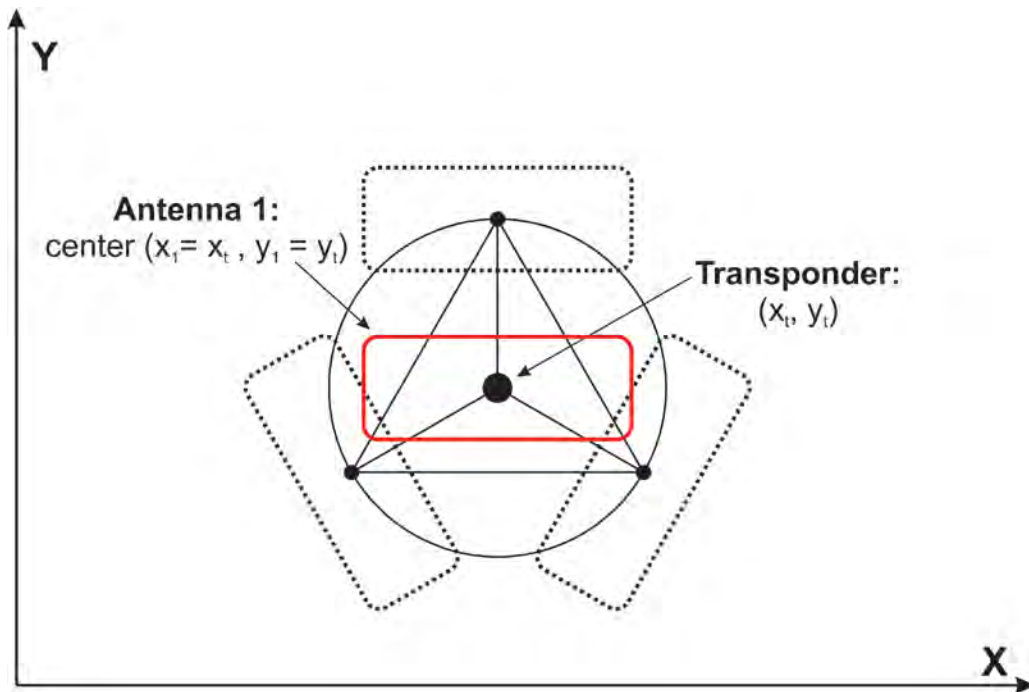


Figure 1-15. Schematic representation of the applied triangulation method to locate the position of the buried transponder in the 3-D domain, by raising the excitation antenna right above the plane location of the transponder.

1.3.2.2 Field experimental setup

Experimental series #	Experimental description	Number of runs
F1	Development of a custom made excitation antenna	12
F2	RF signal strength calibration curves developed in the field	10

Table 1-3. Summary of the “field” experiments performed.

1.3.2.2.1 Development of a custom made excitation antenna

The thrust of the work here is the development of a custom excitation antenna to increase the maximum antenna-transponder detection distance (Figure 1-16). The maximum detection distance is a function of more than one parameters, namely (i) the reader transmitted power, (ii) the physical dimensions of the excitation antenna, (iii) the size of the transponder inner antenna, (iv) the transponder orientation with respect to the excitation antenna plane, (v) the medium in between the excitation antenna and the transponder, (vi) the transponder housing material and (vii) the level of noise in the surrounding environment (Papanicolaou et al. 2010; Li et al. 2011). From all these parameters, the reader's transmitted power is fixed, while the transponder inner antenna is limited by the system configurations considered. The transponder orientation, the type of the material found in between the antenna and the transponder, as well as the transponder housing material are determined by the nature of the application. The construction of a custom excitation antenna allows the user not only to considerably increase the maximum antenna-transponder detection distance, but also to manipulate the size and shape of the antenna according to the specific requirements of each monitoring site (Hassan and Chatterjee 2006; Dziadak et al. 2009).

The antenna inductance (L) signifies its ability to store energy within the created electromagnetic field and its units are in Henry (H). For the case of the TI RFID system specifications, the antenna inductance should not exceed 80 μH (TI Series 2000 Reader System Reference Guide, 2008). The antenna inductance is given by the formula:

$$L = \frac{1}{4\pi^2 f^2 C} \quad (3 - 7)$$

where f is the RFID system frequency (134 kHz); and C is the resonance capacitance (Farad). The resonance capacitance can be achieved by connecting the antenna tuning board capacitors

- **The antenna inductance (L) signifies its ability to store energy within the created electromagnetic field.**
- **The antenna quality factor (Q) indicates the strength of the generated electromagnetic field.**
- **The excitation antenna electromagnetic field strength (H) generated by the charge supplied by reader to the excitation antenna, is a measurement that shows the maximum distance at which the antenna can successfully activate a transponder.**

either in parallel or in series via a set of jumpers (TI Series 2000 Reader System Reference Guide, 2008).

The antenna quality factor (Q) is another important antenna parameter that can affect its performance in terms of the strength of the generated electromagnetic field. Q quantifies the bandwidth of the RF signal, as well as the sharpness and selectivity of the circuitry and is dependent on the inverse of the antenna's resistance (R). One direct way to manipulate Q is by selecting the appropriate wire gage. In this study, three different wire gages were tested, namely AWG 12, AWG 14 and AWG 18 respectively. The antenna efficiency can be computed using the formula:

$$Q_{ant} = \frac{2\pi fL}{R_{ant}} \quad (3 - 8)$$

The above described antenna parameters (i.e., antenna inductance, quality factor, resistance) through the produced antenna current (I_{ant}) amperage along with the antenna dimensions expressed through the antenna radius (r_{ant}) will determine the strength of the antenna's electromagnetic field. The formula for calculating the I_{ant} is:

$$I_{ant} = \frac{V_{ant}}{2\sqrt{2}\sqrt{R_{ant}^2 + (2\pi fL)^2}} \quad (3 - 9)$$

where V_{ant} is the antenna voltage measured at the antenna cable connectors (Volts).

The excitation antenna electromagnetic field strength (H) generated by the charge supplied by reader to the excitation antenna, is a measurement that shows the maximum distance at which the antenna can successfully activate a transponder. As the transponder is moved away from the center of the antenna, the strength of the field decays with distance in the minus three power (d^{-3}), which is well established in the literature (Finkenzeller 2010). The field strength of an antenna at a distance d is calculated by the formula:

$$H = \frac{n_{ant}r_{ant}^2I_{ant}}{2(d^2 + r_{ant}^2)^{1.5}} \quad (3 - 10)$$

where n_{ant} is the excitation antenna windings.

The strength of the magnetic field is given by

$$B_{coil} = \frac{\mu \times N \times I}{2 \times \Lambda} \quad (3-11)$$

where μ is the effective permeability of the coil;
 A is the cross-sectional area of the coil; and
 Λ is the length of the coil-solenoid.

Having determined all the antenna parameters that affect the antenna’s electromagnetic field strength, the “theoretical” maximum antenna-transponder detection distance ($D_{a-t,max}$) can be calculated using the excitation antenna electromagnetic field strength formula combined with the minimum level of energy that the transponder requires in order to be activated (Personal communication with TI engineers).

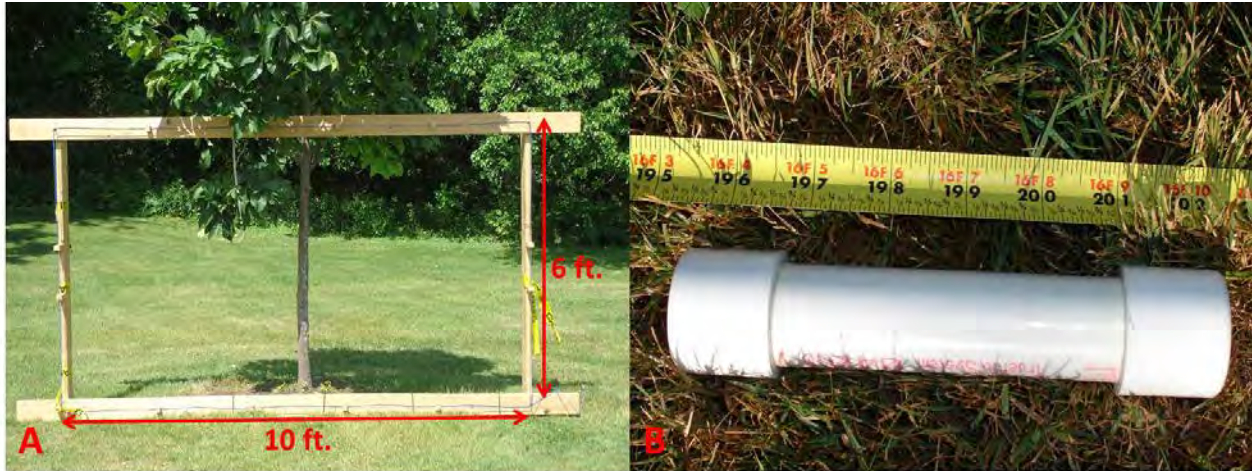


Figure 1-16. (A) Custom excitation antenna’s performance evaluation setup and (B) PVC encased transponder developed by TI.

1.3.2.2.2 RF signal strength calibration curves developed in the field

Limited field experiments were conducted at the Willow Creek Park in Iowa City, IA, a quarry located in Coralville, IA, as well as the Clear Creek in Camp Cardinal, IA. The purpose of designing these experimental series was to develop RF signal strength calibration curves in different mediums (i.e., air, sand and gravel) under field conditions using the custom made excitation antenna (antenna dimensions $3 \times 1.83 \text{ m}^2$), as well as to evaluate the performance of the TI LF, passive RFID system in real field applications. Willow Creek Park was selected due to the fact that the electromagnetic interference from the surrounding environment was minimal and therefore was an ideal place to develop the RF signal strength calibration curves in air (Figure 1-17). The transponder was attached to a wooden pole and a level was mounted to ensure that the transponder was oriented perpendicular to the excitation antenna plane at all times. Also, some preliminary RF signal strength calibration curves were developed for sand and gravel mediums. A specially designed wooden structure with PVC pipes, cut lengthwise, attached to it was built to accommodate the different mediums considered herein (i.e., sand and gravel) and the transponder (Figures 1-18a and 1-18b). Special care was taken to ensure that the wooden structure was perpendicular with respect to the excitation antenna plane at all times. For each medium used, the maximum antenna-transponder detection distance was recorded and measurements were taken at 1-foot increments.

The sand medium experiments were further replicated at a quarry environment, where huge piles of sand were available. An 18 ft. deep hole was drilled to facilitate the transponder (Figure

1-19). A plastic chain was attached to the transponder to allow the upward movement and the recovery of the transponder after the measurements were taken. Once the transponder was placed at the end of the 18 ft. deep hole, the hole was packed with material to ensure that the transponder was fully covered with sand.

In order to evaluate the performance of the TI LF, passive RFID system, four transponders were installed at different depths (2, 4, 8 and 12 ft.) below the channel bed of Clear Creek near Camp Cardinal in Johnson County, IA (Figure 1-20). The transponders were driven into the streambed by simply hammering a PVC tube into the bed, by hand, with the transponders attached to a chain and then removing the tube (Figure 1-21). The use of a vibracore was also tested for feasibility and proved useful but at times cumbersome. Measurements of the RF signal strength between the buried transponders and a floatable, PVC encased custom made antenna were obtained during two visits to the field site, before and after a major flood event to test the system ability to capture scour. For each transponder, ten measurements were collected for repeatability and additional statistical analysis of the data. Figure 1-22 shows the field setup specially developed for a riverine environment. **Each installed transponder had been assigned with a unique Serial Number (S/N) and information regarding its burial depth and its location coordinates were stored into its memory.** The locations of the buried transponders were recorded using a RTK GPS with accuracy of 2 cm to easily find their burial locations at the second visit after the flood.

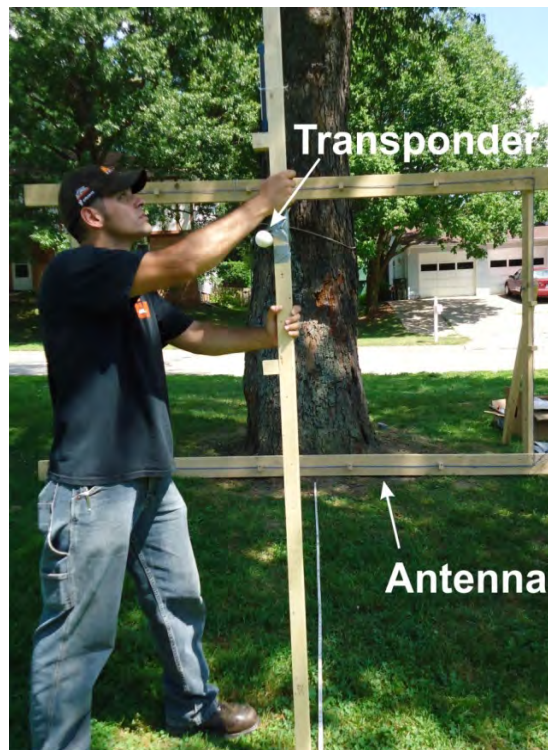


Figure 1-17. Willow Creek Park experimental setup for developing RF signal strength calibration curves in air.

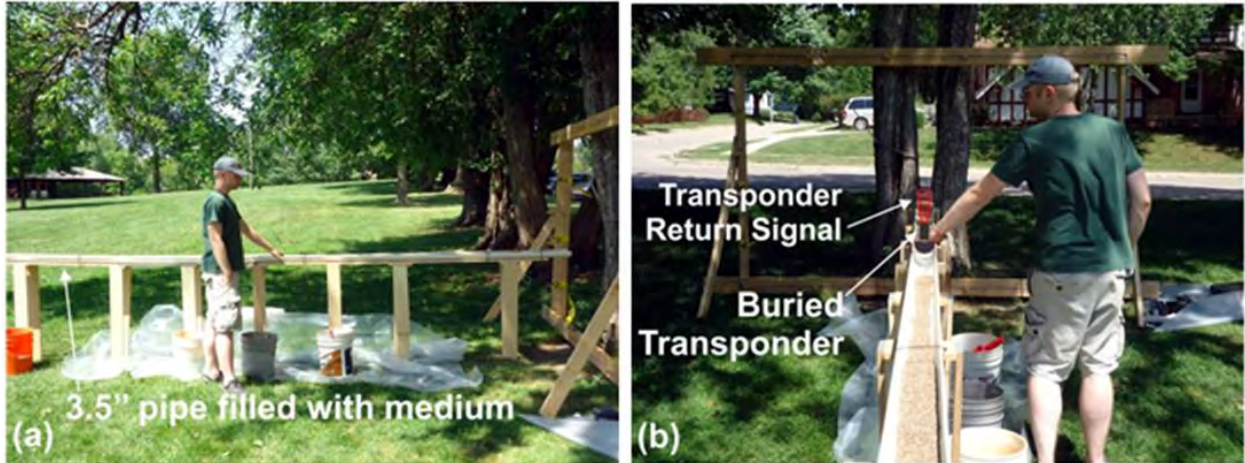


Figure 1-18. Willow Creek Park experimental setup for developing RF signal strength calibration curves in sand and gravel mediums. (a) Side view of the experimental setup with the wooden structure and the PVC pipes on top of it and the custom made excitation antenna and (b) Filling the PVC pipes with material to bury the transponder.

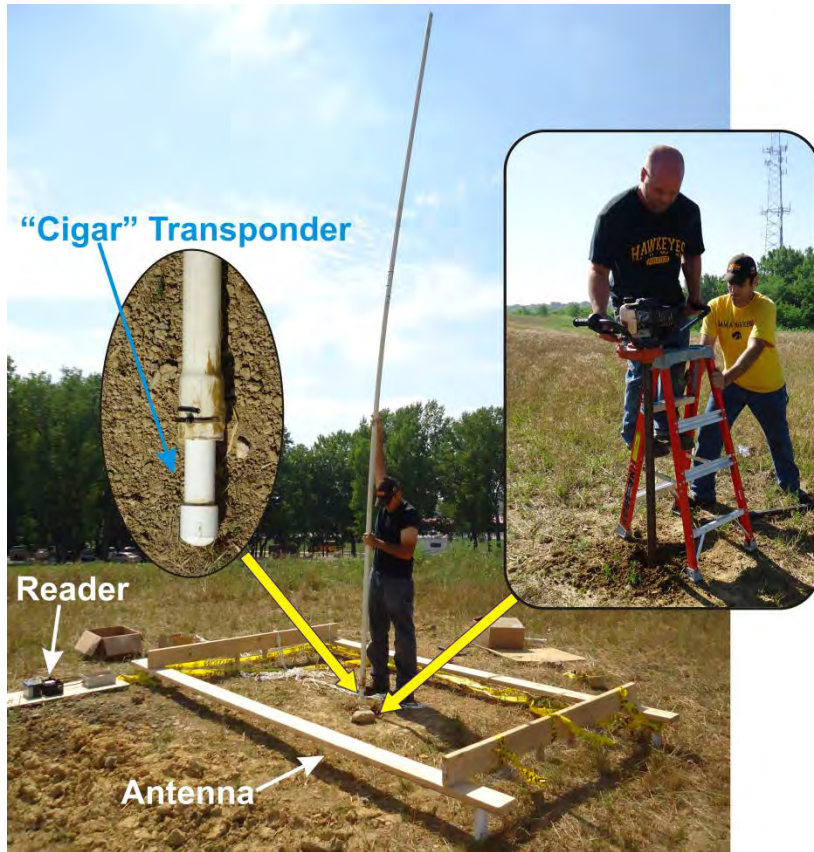


Figure 1-19. Quarry RFID experimental setup. A 18 ft. deep hole was drilled to place the transponder.



Figure 1-20. RFID transponders' installation location in Clear Creek near Camp Cardinal in Johnson County, IA (location coordinates: 41°40'35" N and 91°35'55" W).



Figure 1-21. Transponder stream bed installation process setup.



Figure 1-22. Field monitoring setup to obtain the RF signal strength of each transponder.

1.4 Transponder's return RF signal strength analysis (RSSI)

The RF signal (in voltage) consists of three main parts. The first part or the big “plateau” (V_c) (indicated with the red color in Figure 1-23) corresponds to the transponder “charging” part and represents the energy required to activate the circuitry of the transponder. The energy is transferred from the reader to the transponder through the electromagnetic field of the excitation antenna and it is approximately 3 volts. This amount of energy is required to power up the inactive passive transponder in order the transponder to send back to the reader a response RF signal (TI Antenna Reference Guide 1996). This part of the RF signal lasts approximately 0.050 seconds (Figure 1-23) and during this time length the reader is in the “sending” mode, while the transponder is in the “listening” mode. The second part of the RF signal is the transponder return RF signal (V_r) or the “step” part of the RF signal (indicated with the cyan color in Figure 1-23) which corresponds to the transponder response to the reader interrogation request RF signal. The transponder uses the energy stored in the excitation antenna’s electromagnetic field to charge its circuitry and send back a replied RF signal to the reader. The voltage of the transponder return RF signal is reduced, since a part of the initially received energy was consumed to activate the transponder. The transponder return RF signal time duration is approximately 0.016 seconds (Figure 1-23) and during this time length the transponder is in the “sending” mode, while the reader is in the “listening” mode. Finally, the last part of the RF signal or the “oscillating” part (indicated with the green color in Figure 1-23) represents the synchronization process between the reader and the interrogated transponder at which the reader is trying to establish the line of communication with the transponder. The time duration of this part is approximately 0.030 seconds (Figure 1-23) and for this time length the reader is in the “sending” mode while the transponder is in the “standby” mode.

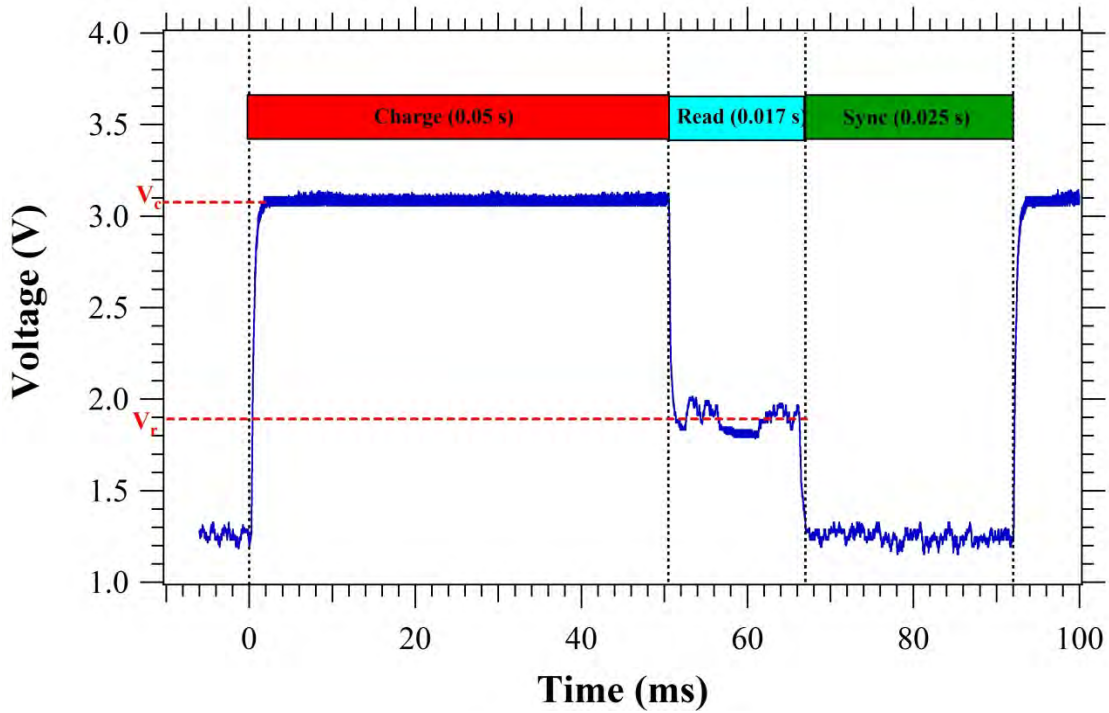


Figure 1-23. One RF signal cycle (~ 0.1 seconds) main parts and time lengths.

For each measurement point (i.e., point #1, point#2...) (Figure 1-24), the RF signal strength was calculated by the formula:

$$\text{Signal Decay (\%)} = \left(\frac{V_c - V_r}{V_c} \right) \times 100\% = \left(1 - \frac{V_r}{V_c} \right) \times 100\% \quad (3 - 12)$$

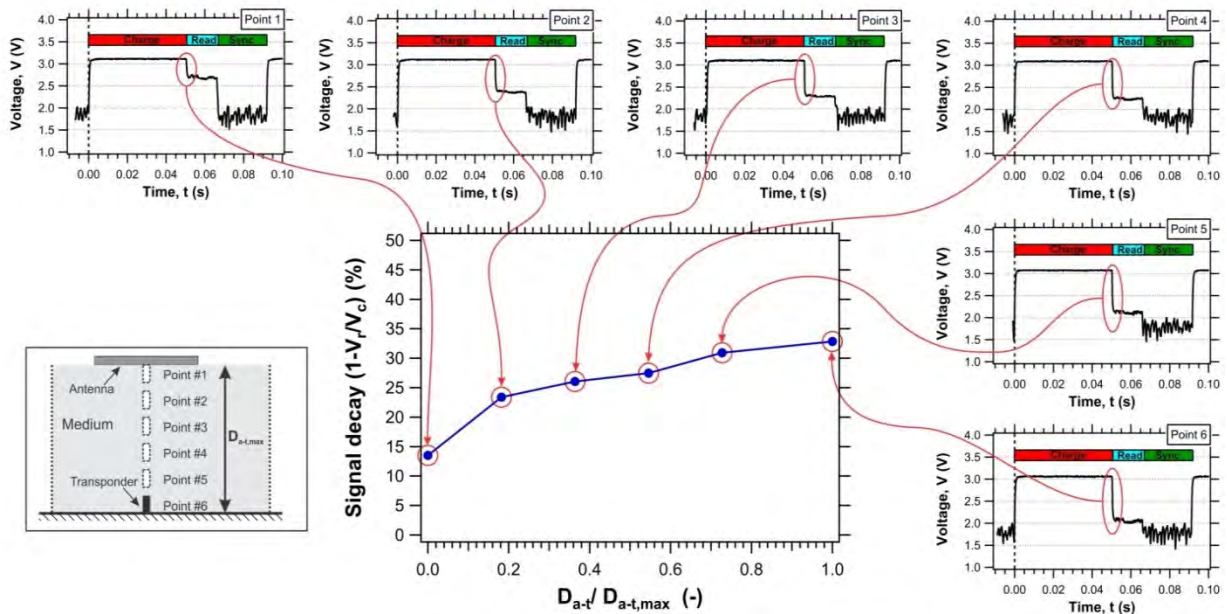


Figure 1-24. Development of RFID reader voltage vs. antenna-transponder distance calibration curves.

2. RESULTS

This section of the report describes the findings of the laboratory and field experiments to address the project goals (deliverables). First, the laboratory results are presented focusing on exploring the potential of the TI LF, passive RFID system in a controlled environment, followed by the findings from the field experiments, where the overall RFID system performance is tested and evaluated. Table 2-1 summarizes the components of the proposed RFID system which will be used for developing a robust and reliable system to monitor scour depth around hydraulic structures.

2.1 Laboratory results

2.1.1 Transponder housing experiments

The maximum detection distance between the excitation antenna and the transponders was determined from iterative experiments where the transponders were encased into “rock” and “concrete” housing material and compared with a “naked” transponder. The antenna-transponder distance increased until the communication between the excitation antenna and the transponder was lost. The point at which the communication was no longer feasible was considered as the maximum antenna-transponder detection distance. Figure 2-1 presents the antenna-transponder maximum detection distance occurred for each housing material considered herein, after the excitation antenna was swept over the transponders 16 times providing a total of 48 iterations to detect the transponders.

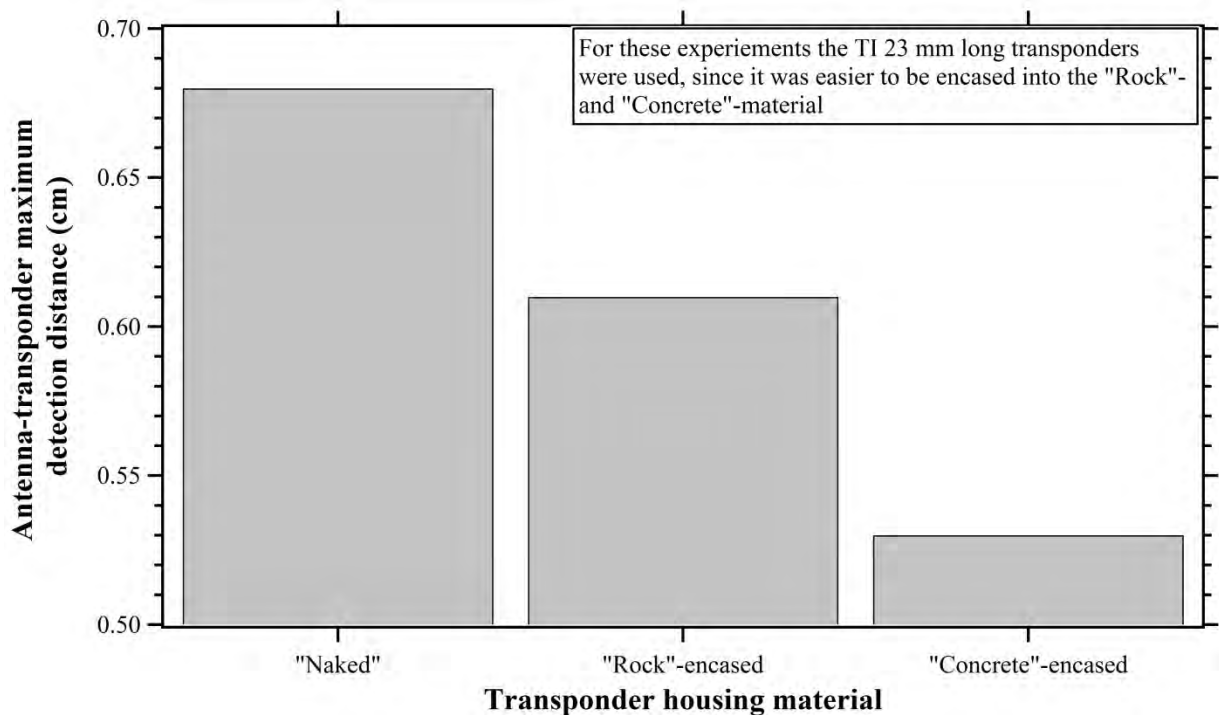


Figure 2-1. Antenna-transponder maximum detection distances for different transponder housing material (i.e., “naked”, “rock”- and “concrete”- encasement) after a total of 16 iterations.

Component	Specification
Reader	Radio module
	Control module
	Four (4) (Antenna tuning circuits) per reader
	Multiplexer circuit board
	Multiplexer wiring harness
	Datalogger circuit board
	Bluetooth serial adapter
	Serial cable
	Piezoelectric buzzer per reader
	Reader waterproof enclosure (box)
	Four (4) antenna tuning circuit waterproof enclosures (boxes) per reader
	Reader control software
	110V Power supply
Marine battery	Size 34M
Solar power charger for marine battery	55 Watt Solar Panel
	Charge Controller
	Ground/Roof Tilt Mount 02
	Freight
Custom board for signal strength output	-
Antennas	Antenna wiring (for 3x1.8 m loop-estimated)
	Twinax cable between reader and antenna (76 m loop)
120 mm Transponders	Read/write
Inductance meter	-
Tuning indicator	by TI
Wireless data download system	Satellite transmitter
	GPS antenna and cable, Threaded pipe, NU-RAIL fitting
	Datalogger
	Right-Hand Circular Polarized (RHCP) antenna with mounting hardware
	Antenna cable
	Antenna accessories to punch holes for the antenna cables
	24 Ahr battery back, regulator and 20W solar panel

Table 2-1. Components of the proposed RFID system.

As the results indicating, the minimum antenna-transponder detection distance was encountered when the concrete housing material was employed. In this case, the detection distance dropped to 13.1 and 15.88% compared to the “naked” and the “rock”-encased transponders, respectively. On the other hand, the “rock” – encased transponder performed much better compared to the “concrete”-encased transponder, but still the antenna-transponder detection distance occurred was reduced by 10.3% compared to the “naked” transponder. In a nutshell, the results from these experiments showed that the transponder housing material affects the maximum antenna-transponder detection distance and the housing material should be taken into consideration at the design part of the project.

2.1.2 Transponder orientation effects on the transponder return RF signal

The medium considered for assessing the transponder orientation effects on its detectability was air. Results from the 15 different orientation tests showed that the maximum detection distance occurred when the transponder’s long axis was oriented perpendicular to the excitation antenna plane, which hereafter is referred to as the “favorable” transponder orientation. In this case, the intensity of the electromagnetic field created by the transponder obtained its highest value. On the contrary, when the transponder long axis was oriented parallel to the excitation antenna plane (defined here as the “unfavorable” transponder orientation), the minimum antenna-transponder detection distance was recorded. In that latter case, the average detection distance between the excitation antenna and the transponder decreased by 37%. As expected, different in-between transponder orientation positions provided intermediate detection distances, which were bounded between the minimum and maximum values of the excitation antenna detection distance (Figure 2-2). A similar finding has been reported in the literature by Nichols (2004), Allan et al. (2006) and Papanicolaou et al. (2010).

As part of the orientation experiments we have further analyzed the transponder detectability performance by examining the success rate in detecting the transponder for the favorable orientation condition only. In other words, we have not only examined if the transponder was detectable, but also how many times it became detectable. That is the success rate of detection which is evaluated here for different configurations.

We have recorded the detection success rate of four identical transponders. As a matter of fact, we have tested the detection limits and success rate of the RFID system for distances even greater than the ones provided by the manufacturer (i.e., $D_{a-t,max} \sim 0.6$ m). The four transponders were placed at identical distances each time from the excitation antenna and numbered as transponders 1, 2, 3 and 4. They were spaced apart at all times by 0.38 m. The variability in the detection distance for each transponder was recorded by performing 16 sweeps per each chosen distance. The number of times the transponders were detected at different distances - averaged over the 16 sweeps – provides the success rate and is illustrated in Figure 2-3 in the form of % bars. The transponders can be successfully detected 100% of the time, when the antenna–transponder distance is $D_{a-t,max} \sim 0.6$ m. The success rate of detection dropped, as expected, when the antenna–transponder distance became greater than 122% of $D_{a-t,max}$. Nonetheless and to our surprise, the detection success rate remained relatively high in spite of the fact that the transponders distance surpassed the detection range reported by the manufacturer. Please note that for a distance greater than 122% of $D_{a-t,max}$, the RF signals between the excitation antenna

and transponders 1 and 3 were completely lost due to the interference of the electromagnetic fields created by the transponders' internal antennas as they were found at a close proximity to each other (~0.38 m).

In a nutshell, the results of this section show that the transponder orientation does affect the antenna-transponder detection distance and for the favorable orientation position the maximum detection distance reported by the manufacturer can be exceeded by nearly 22%. In this case, the detection success rate dropped down to 63%. That implies that out of the 100 detection attempts, the transponder was detected 63 times. At $D_{a-t,max}$, the transponders can be successfully detected 100% of the time.

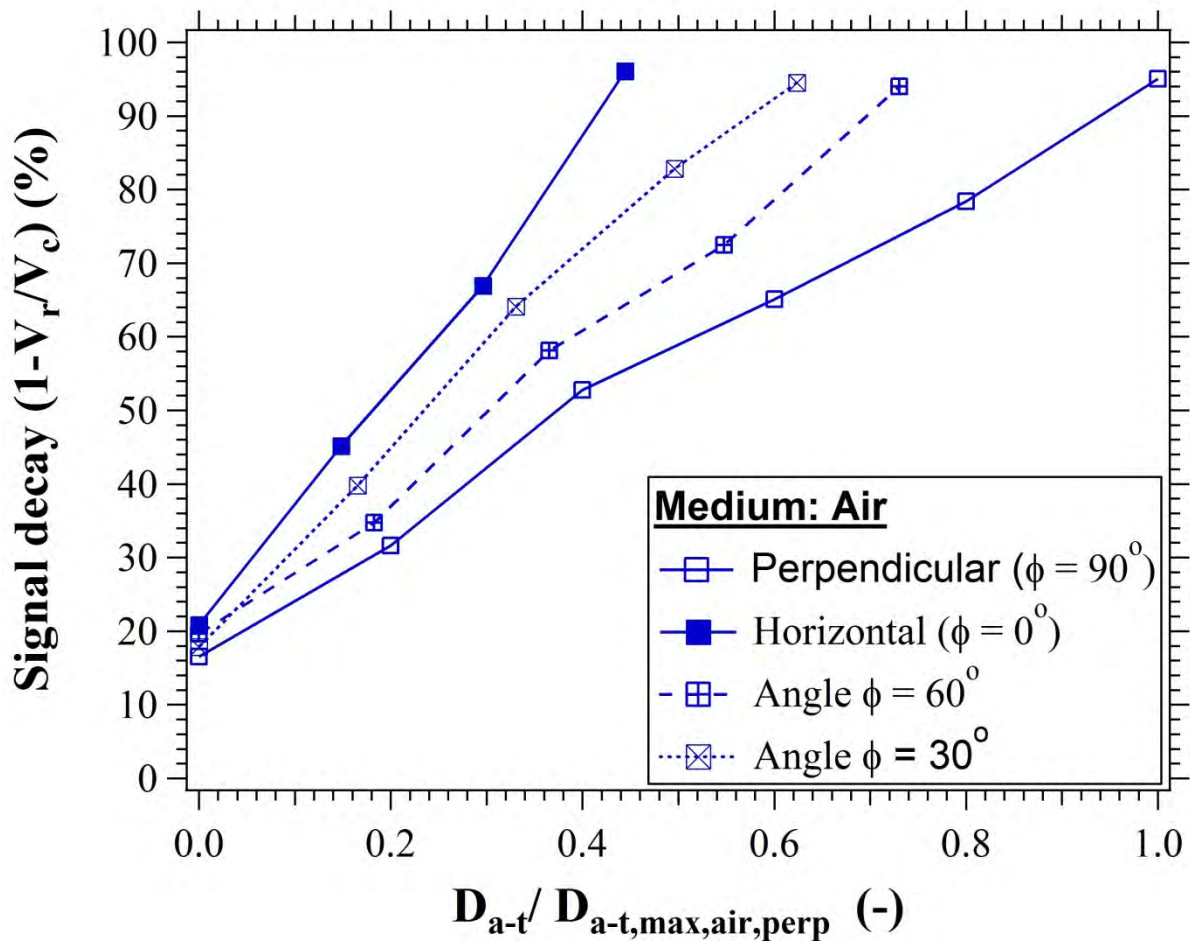


Figure 2-2. Medium and orientation effects (i.e., $\phi = 90, 0, 60$ and 30° transponder long axis orientation with respect to the excitation antenna plane) on the transponder return RF signal strength (RSSI) in air.

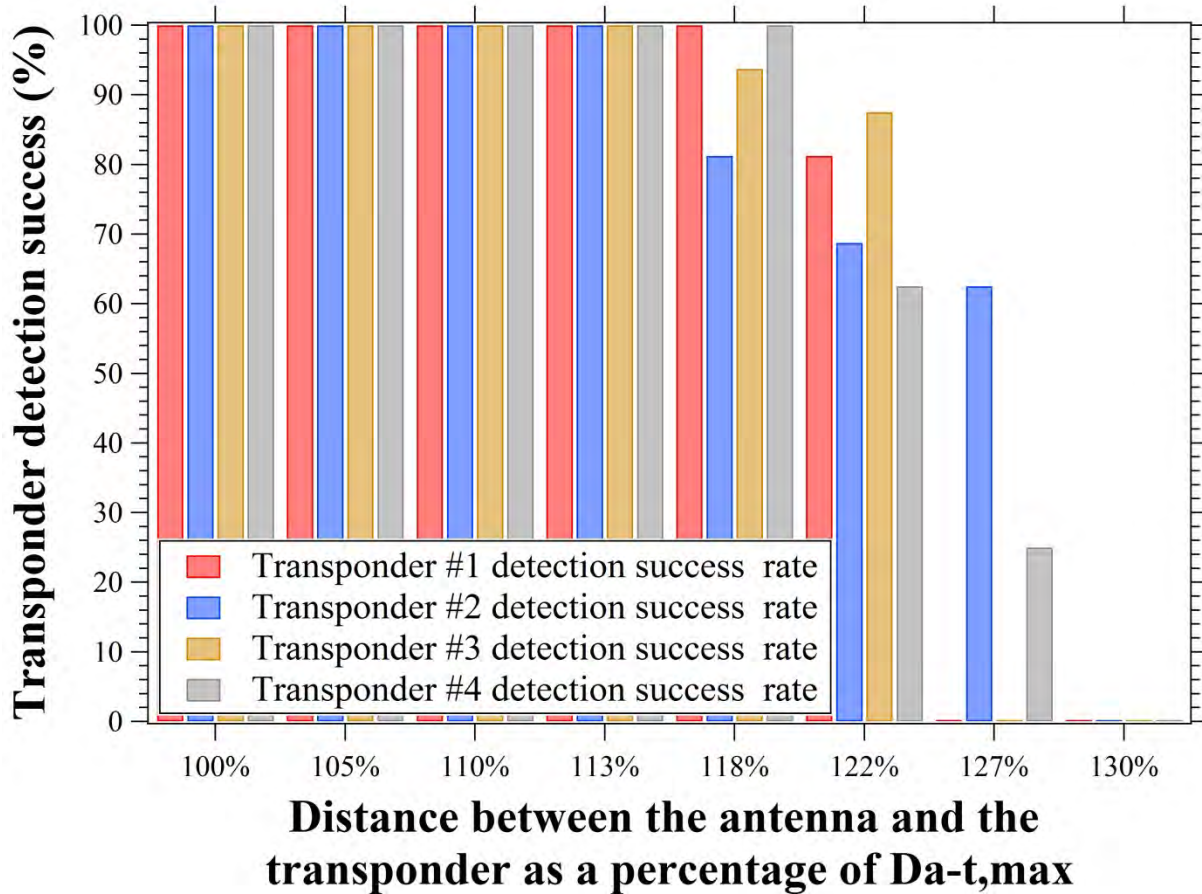


Figure 2-3. Transponder detection success percentage rate as a function of the antenna-transponder distance, for each transponder used in this experimental series.

$$\text{Signal Decay (\%)} = 18.757 + 75.991 \times \frac{D_{a-t}}{D_{a-t,air,max}} \quad (3-13)$$

2.1.3 Medium effects on the RF signal strength decay (RSSI)

In these experiments, the maximum antenna-transponder detection distance of 2 m achieved in air per the manufacturer was compromised by the dimensions of the experimental setup (barrel) which were set here as the maximum detection distance with $D_{a-t,max} = 1.50$ m. Figure 2-4 demonstrates the transponder's return RF signal strength decay curves developed for different material types, namely, air, water, sand and gravel.

When air was the medium, the transponder's return RF signal strength suffered the minimum losses (Figure 2-4) compared to water, sand and gravel mediums. This behavior was expected, as there is no reflection of the signal in air.

In the case of water (Figure 2-4), the maximum antenna-transponder detection distance matched the $D_{a-t,max}$, although the decay rate of the transponder return RF signal strength in water was higher, but still comparable to the one for air. The transponder's return RF signal strength decay curve followed the same linear pattern of that for air.

In the case of gravel (Figures 2-4), the transponder's return RF signal strength decay curve also followed the linear decay pattern similar to the one for the air and water mediums. In this case, the maximum antenna-transponder detection distance matched the $D_{a-t,max}$ and the rate of decay of the transponder's return RF signal strength for gravel was similar to the one for water, except for the closest point to the excitation antenna (25% of $D_{a-t,max}$), where the RF signal strength decay was significantly higher.

Finally, in the case of sand (Figures 2-4) the maximum antenna-transponder detection distance dramatically decreased. In this case, the maximum antenna-transponder detection distance dropped to 64% of $D_{a-t,max}$ and the decay rate of the transponder's return RF signal strength was much higher than the ones corresponded to the other mediums considered herein (as seen in Figures 2-4 the slope of the decay curve for sand was much steeper than the ones for air, water and gravel).

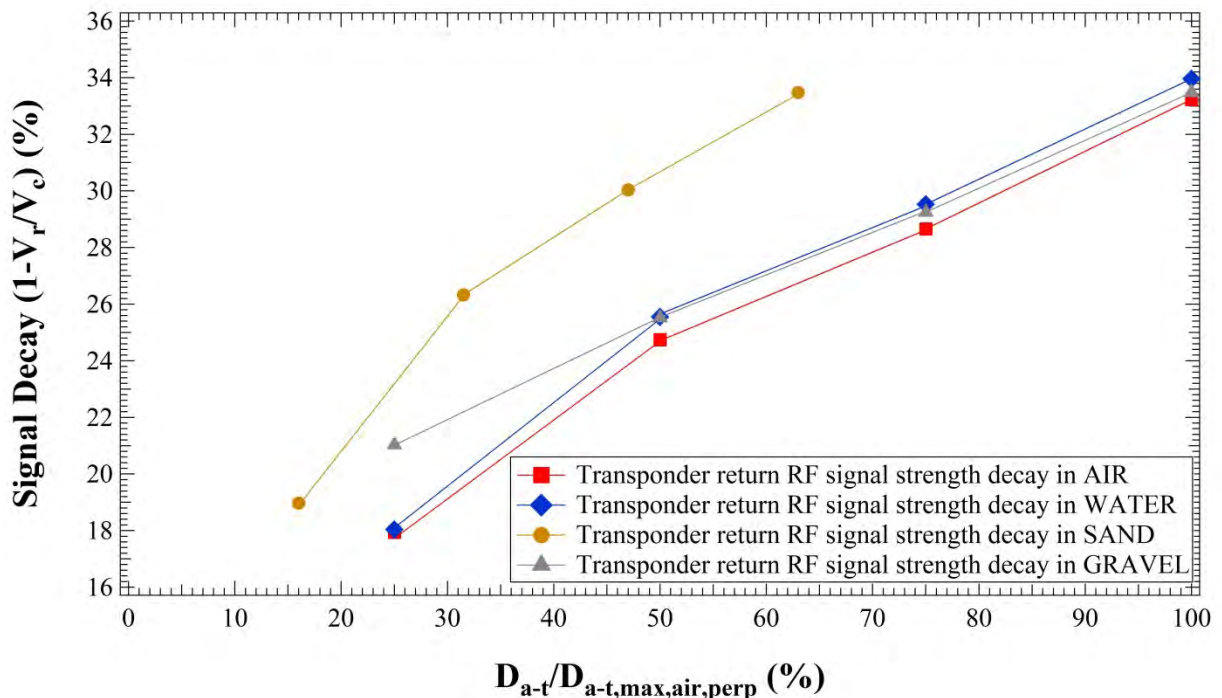


Figure 2-4. RF signal strength decay curves developed in different mediums in between the excitation antenna and the transponder (i.e., air, water, sand and gravel) for the favorable transponder orientation (i.e., $\varphi = 90^\circ$ with respect to the excitation antenna plane).

For each medium considered herein (i.e., water, sand and gravel), the RF signal strength curve was developed for different transponder's long axis orientations (i.e., $\phi = 90^\circ$, 0° , 60° and 30°) with respect to the excitation antenna plane. Figures 2-5 to 2-7 present the RF signal strength curves developed, grouped in by the medium type in between the excitation antenna and the transponder. The RF signal strength decay curves reconfirmed the findings of the orientation experiments performed in air (see section 4.1.2), where the lowest rate of the RF signal strength decay occurred when the transponder's long axis was oriented favorably towards the excitation antenna plane ($\phi = 90^\circ$) for all the mediums tested (the slope of the corresponding curves was the mildest compared to the other transponder's orientations for each medium), while the highest rate of the RF signal strength decay observed when the transponder's long axis was oriented unfavorably with respect to the excitation antenna plane ($\phi = 0^\circ$). The RF signal strength decay curves for the 60° and 30° transponder long axis orientation lied in between the favorable and unfavorable transponder orientation RF signal strength decay curves, creating an envelope shaped curves. The 60° transponder orientation RF signal strength decay curve was closer to the favorable transponder orientation RF signal strength decay curve ($\phi = 90^\circ$), while the 30° was closer to the unfavorable transponder orientation RF signal strength decay curve ($\phi = 0^\circ$). This envelope shaped curves' pattern was observed for all the mediums tested in this experimental series, indicating that the transponder long axis orientation affects the rate of decay of the RF signal strength and should be taken into consideration in the initial steps of the project design.

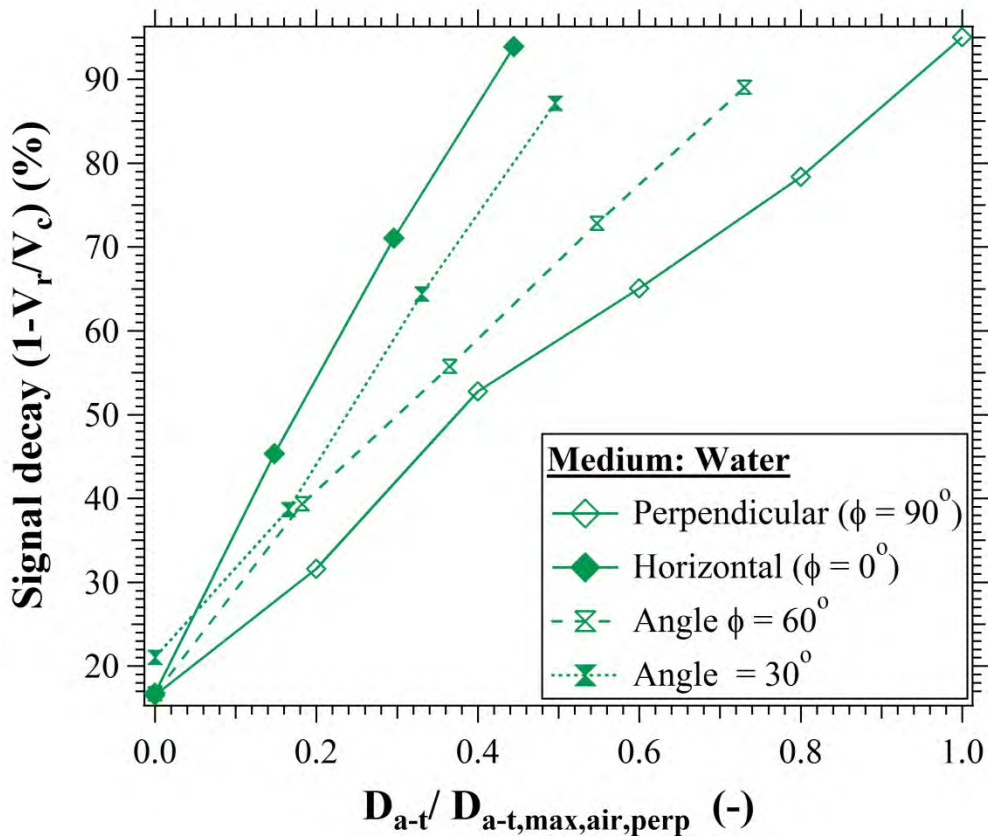


Figure 2-5. Medium and orientation effects (i.e., $\phi = 90^\circ$, 0° , 60° and 30° transponder long axis orientation with respect to the excitation antenna plane) on the transponder return RF signal strength (RSSI) in water.

These findings agree with the results presented by Dziadak et al. (2009), where the shortest antenna-transponder detection distance occurred when the transponder was buried into sand, while the detection distances corresponding to air and gravel were significantly longer. Therefore, the type of medium that is found between the excitation antenna and the transponder affects the maximum antenna-transponder detection distance and can dramatically deteriorate the detection distance and success rate of the RFID system. Dziadak et al. (2009) attributed this drop with the sand medium to the electromagnetic properties exhibited by sand silicate (i.e., magnetic permeability, permittivity, and electric conductivity) which collectively affect the RF signal propagation into the sand medium.

$$\text{Signal Decay (\%)} = 19.025 + 76.010 \times \frac{D_{a-t}}{D_{a-t,air,max}} \quad (3-14)$$

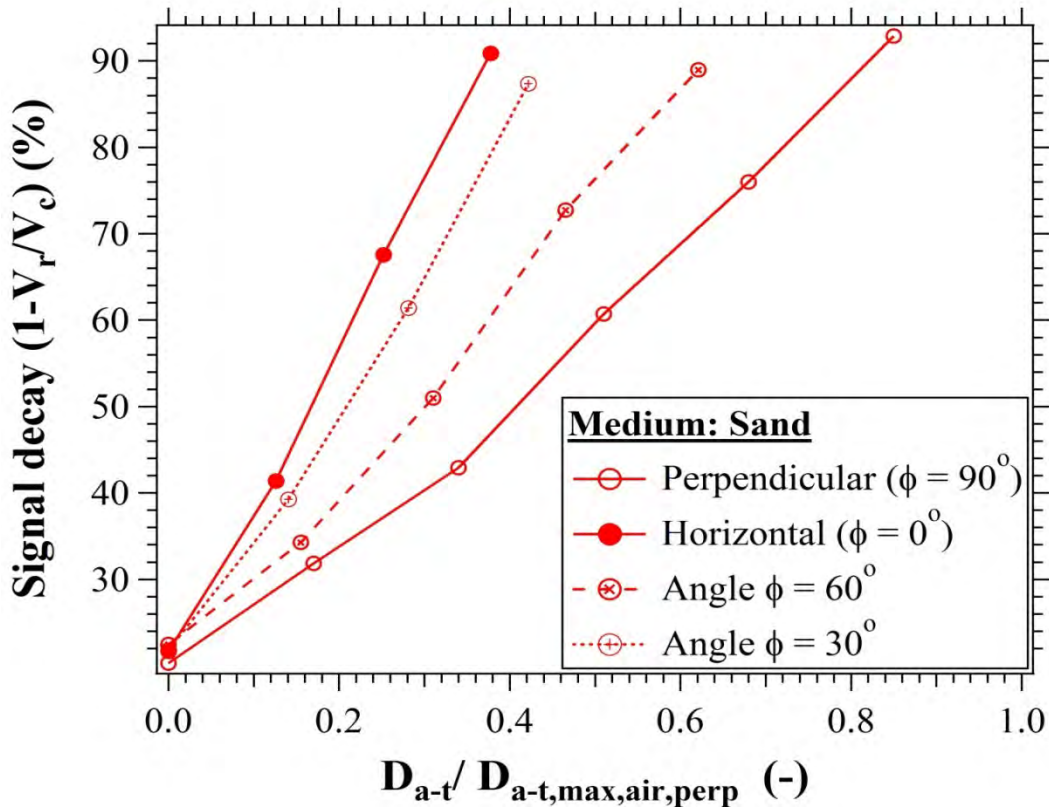


Figure 2-6. Medium and orientation effects (i.e., $\phi = 90, 0, 60$ and 30° transponder long axis orientation with respect to the excitation antenna plane) on the transponder return RF signal strength (RSSI) in sand.

$$20.185 + 67.445 \times \frac{D_{a-t}}{D_{a-t,air,max}}, \text{ for } \frac{D_{a-t}}{D_{a-t,air,max}} < 0.348 \quad (3-15)$$

Signal Decay (%) =

$$8.763 + 100.205 \times \frac{D_{a-t}}{D_{a-t,air,max}}, \text{ for } \frac{D_{a-t}}{D_{a-t,air,max}} > 0.348 \quad (3-16)$$

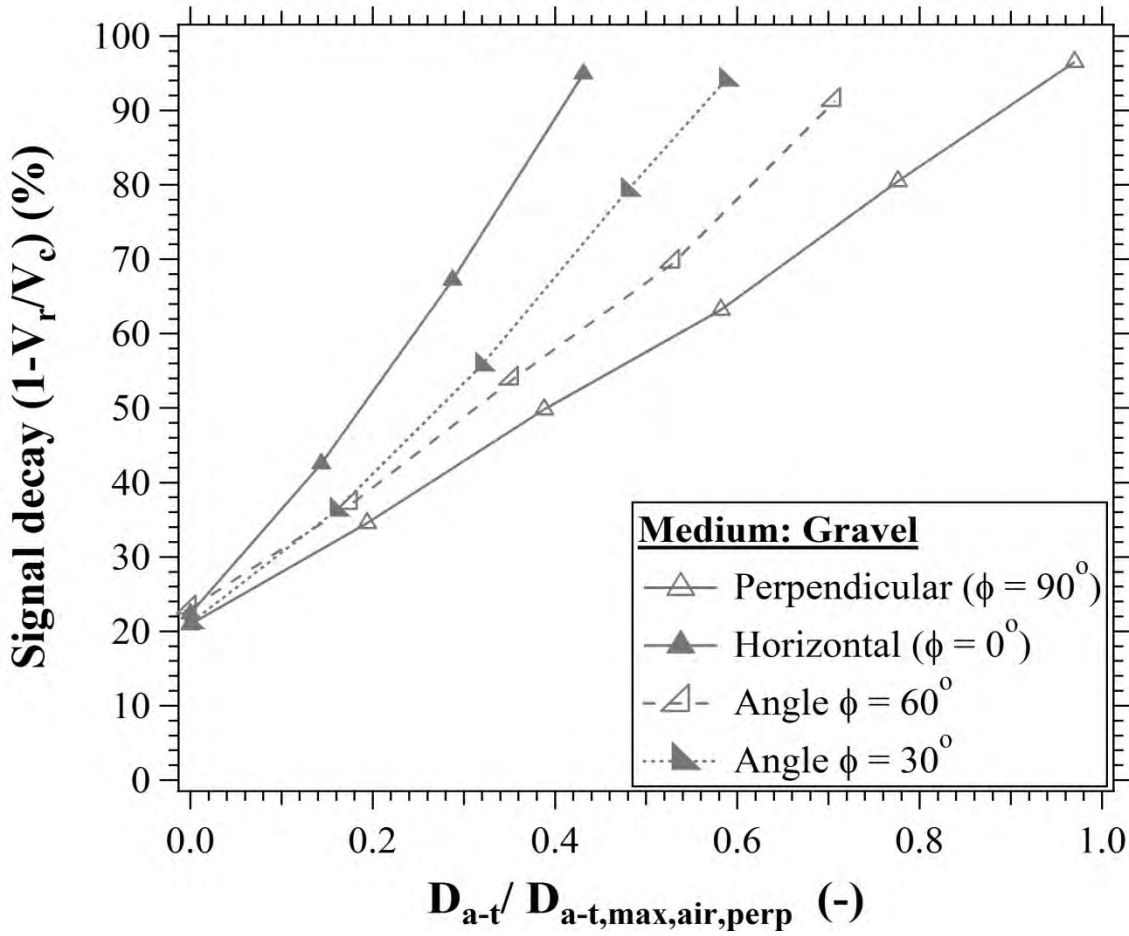


Figure 2-7. Medium and orientation effects (i.e., $\phi = 90, 0, 60$ and 30° transponder long axis orientation with respect to the excitation antenna plane) on the transponder return RF signal strength (RSSI) in gravel.

$$19.200 + 77.361 \times \frac{D_{a-t}}{D_{a-t,air,max}}, \text{ for } \frac{D_{a-t}}{D_{a-t,air,max}} < 0.489 \quad (3-17)$$

Signal Decay (%) =

$$15.219 + 85.502 \times \frac{D_{a-t}}{D_{a-t,air,max}}, \text{ for } \frac{D_{a-t}}{D_{a-t,air,max}} > 0.489 \quad (3-18)$$

2.1.4 Location of the buried transponder in the 3-D domain

The identification of the geospatial (x-y) coordinates of the installed transponders is of primary importance for the success of this project, since the transponder's return RF signal strength (RSSI) is coupled with the distance between the excitation antenna and the transponder. In literature, it has been reported that the RF signal patterns developed between the excitation antenna and a transponder can lead to false conclusions regarding the location of the buried transponder, due to the fact that the outer the interception of the two electromagnetic fields is with respect to the center of the excitation antenna, the higher the RF signal strength decay is, indicating that the transponder is located further away (or deeper in the stream bed in case of scour monitoring) from the excitation antenna than it really is (Dziadak et al., 2008; Dziadak et al., 2009; Kumar and Sommerville, 2012). Therefore, the development of an algorithm that will allow the user to locate the exact position of the buried transponder in the x-y plane is a key component of the RFID scour monitoring system. An algorithm developed in C++ programming language, accepts three GPS coordinates (i.e., longitude and latitude), which are identified by moving the antenna and attached GPS device to the limits of the RF signal emitted by a transponder. These three coordinates form a triangle and using the circumcircle triangle theory (see section 3.2.1.4 for more details) its center can be found using the developed algorithm. This triangulation algorithm transforms the GPS coordinates into Cartesian coordinates.

Once the center is calculated, the Cartesian coordinates are re-transformed back into the GPS coordinates providing the user with the exact location of the buried transponder in the x-y plane (Figure 2-8). The accuracy of the triangulation algorithm is affected by (i) the accuracy of the GPS tracking device (~ 2 cm) and (ii) the accuracy of placing the excitation antenna at the location where it starts to detect the transponder. After 8 repeated runs and by comparing the triangulation algorithm outputs with the actual transponder's location in the 2D domain, the average deviation of the calculated coordinates was ~ 5.5 cm.

After having successfully identified the exact location of the buried transponder in the x-y plane, the user should place the excitation antenna right above the calculated location of the buried transponder and record the transponder's return RF signal strength (RSSI). By comparing the obtained RSSI value with the RF signal strength decay curve developed specifically for the medium that the transponder is buried, the user can easily calculate the transponder's burial depth and its position in the 3D domain. The accuracy of this step highly depends on the accuracy of the calculated transponder's coordinates in the 2D domain (previous step). The average deviation of the transponder's calculated burial depth from the original based on the 8 experimental runs performed herein was found to be ~ 4 cm.

```

Y:\WSDOT\TriangulationCode.exe
Please pass the GPS coordinates for the first point
Latitude Point #1
degrees:
38
North (N) or South (S)?
N
Minutes & Seconds:
0110
Longitude Point #1
degrees:
96
West (W) or East (E)?
W
Minutes & Seconds:
5742
Please pass the GPS coordinates for the second point
Latitude Point #2
degrees:
38
North (N) or South (S)?
N
Minutes & Seconds:
0710
Longitude Point #2
degrees:
96
West (W) or East (E)?
W
Minutes & Seconds:
5108
Please pass the GPS coordinates for the third point
Latitude Point #3
degrees:
38
North (N) or South (S)?
N
Minutes & Seconds:
0410
Longitude Point #3
degrees:
96
West (W) or East (E)?
W
Minutes & Seconds:
5442
The centre of the circle, where the RFID transponder is located, is: (3232.24,
847.148)
Press any key to continue . . .

```

Figure 2-8. Screenshot of the triangulation code, requiring the user to insert the 3 antennas GPS coordinates to calculate the location of the buried transponder in the x-y plane (2D domain).

2.2 Field results

2.2.1 RF signal strength calibration curves developed in the field

The successful performance of the TI LF (134.2 kHz), passive RFID technology to remotely monitor scour in a laboratory environment, along with its relatively low cost, motivated us to examine its applicability in the field, under real conditions. This field experimental series are based on the interesting findings from the laboratory results, where (i) the distance between the excitation antenna and the transponder determines the RF signal strength and (ii) the type of the medium in between the excitation antenna and the transponder affects the rate of decay of the RF signal strength. The following describes the field results conducted first at the Willow Creek Park in Iowa City, IA, and a quarry located in Coralville, IA, and then a real case, where the transponders were installed into the stream bed of Clear Creek in Camp Cardinal, IA.

The first part of this experimental series was designed to test and evaluate the performance of the TI LF (134.2 kHz), passive RFID system along with the custom made excitation antenna by developing RF signal strength decay curves in various mediums (i.e., air, water, sand and gravel) for the favorable transponder orientation with respect to the excitation antenna plane.

Figure 2-9 presents the RF signal strength decay curves with distance between the excitation antenna and the transponder for air (blue color), water (green color), sand (red color) and gravel (grey color). Overall, the RF signal strength decay curve in air performed the best, since the TI RFID system is developed to operate in air. The RF signal strength decay curves in water and gravel performed quite similar to the decay curve in air, however, the standard error was consistently higher for the gravel and water mediums compared to air, indicating that there is variability due to the medium at which the RF signal travels through. The RF signal strength decay curve developed for sand is described by a higher decay rate (steeper slope) compared to the other RF signal decay curves considered herein, while the antenna-transponder maximum detection distance achieved was reduced by 15% compared to the ones observed for the other mediums. The RF signal strength curves follow an approximately linearly decaying pattern, as the distance between the excitation antenna and the transponder increased. The correlations values, r^2 , of the RF signal strength decay curves are close to unity (~ 0.995), indicating a strongly linear relationship between the decay of the RF signal strength and the distance. This linear trend was expected since it is already known from the electromagnetic theory that the RF signal strength linearly attenuates with the square of the distance traveled from the source. This linearly decaying pattern of the RF signal strength with distance is further supported by the findings of Ko 2010, where they plotted the RF signal strength in dBm (decibels) with distance between the excitation antenna and the transponder. In Barralet et al. (2009) study, they plotted the RSSI with the distance in logarithmic scale, in order to obtain a linear relationship, since dBm is a logarithmic scale.

The second part of this experimental series was to test and evaluate the performance of the TI RFID system in real field conditions by installing transponders into the stream bed at various depths at a degrading (erodible) reach. Four transponders were installed in the stream bed at depths of 2, 4, 8 and 12 ft., during a low flow event. Once the transponders were installed, the transponder return RF signal strength was recorded via a digital oscilloscope. These measurements were used as baseline conditions to bear comparisons with the RF signal strength values obtained after the major flood event occurred in early June, 2013. For each transponder, ten consecutive measurements were collected for repeatability purposes and further statistical analysis. The measured RF signal strength decay value for each transponder was normalized to the approach flow depth and related to the burial depth of the transponder. The corresponding flow depths on the measurement dates were 1.97 ft. (0.6 m) and 3.07 ft. (0.94 m), respectively. The flow depths directly over the transponders were also measured using the sonar device on each collection date for consistency purposes. The measured scour depth on 06/07/2013 was 2.64 ft. (0.80 m). This measured scour depth was compared to the predicted maximum scour depth using established scour formulae. The Jain and Fischer (1979) formula calculated a maximum scour depth of 12.47 ft. (3.80 m), while the CSU (1975) calculated a scour depth of 6.36 ft. (1.94 m). The resulting errors were 375 and 142%, respectively. These differences highlight the need to develop a robust and reliable system to monitor scour

Figure 2-10 shows the processed the RF signal strength decay curves developed for the four installed transponders corresponding to the two measurement dates. The decay curve for the transponders on 04/05/2013 follows the expected linear pattern indicating little to no scour. Conversely, the decay curve for the transponders on 06/07/2013 shows that the transponder buried initially 2 ft. below the stream bed (marked with the red circle) significantly deviates

from the linear trend indicating an abrupt change in transponder orientation resulting from its exposure due to scour. After the flood event, the 2 ft. installed transponder changed orientation due to excessive scour (erosion), which led to significantly increased RF signal strength decay value. The RF signal strength decay values for the rest of the buried transponders did not significantly change compared to the baseline measurements.

This limited field experiments indicated that the LF (134.2 kHz), passive RFID technology is transferable to the field and has the potential to be employed for scour monitoring studies, promoting the use of this technology for remotely monitoring scour. The promising results of the field experiments warrant future development of the RFID technology.

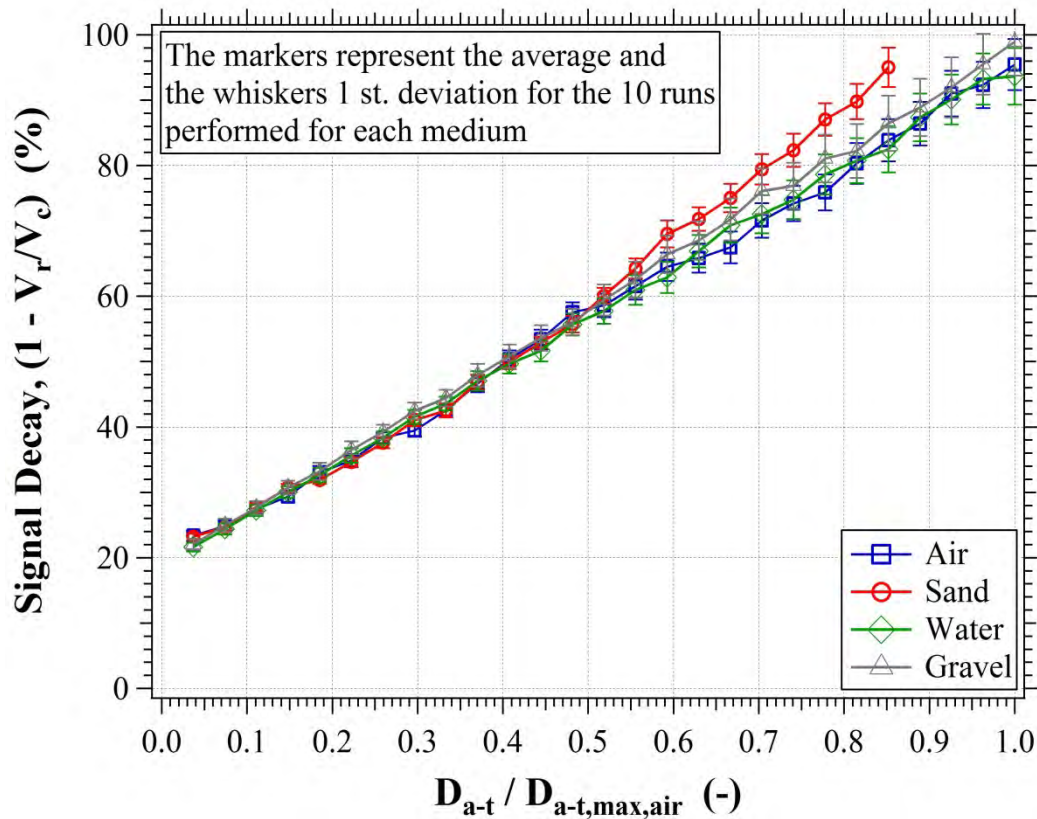
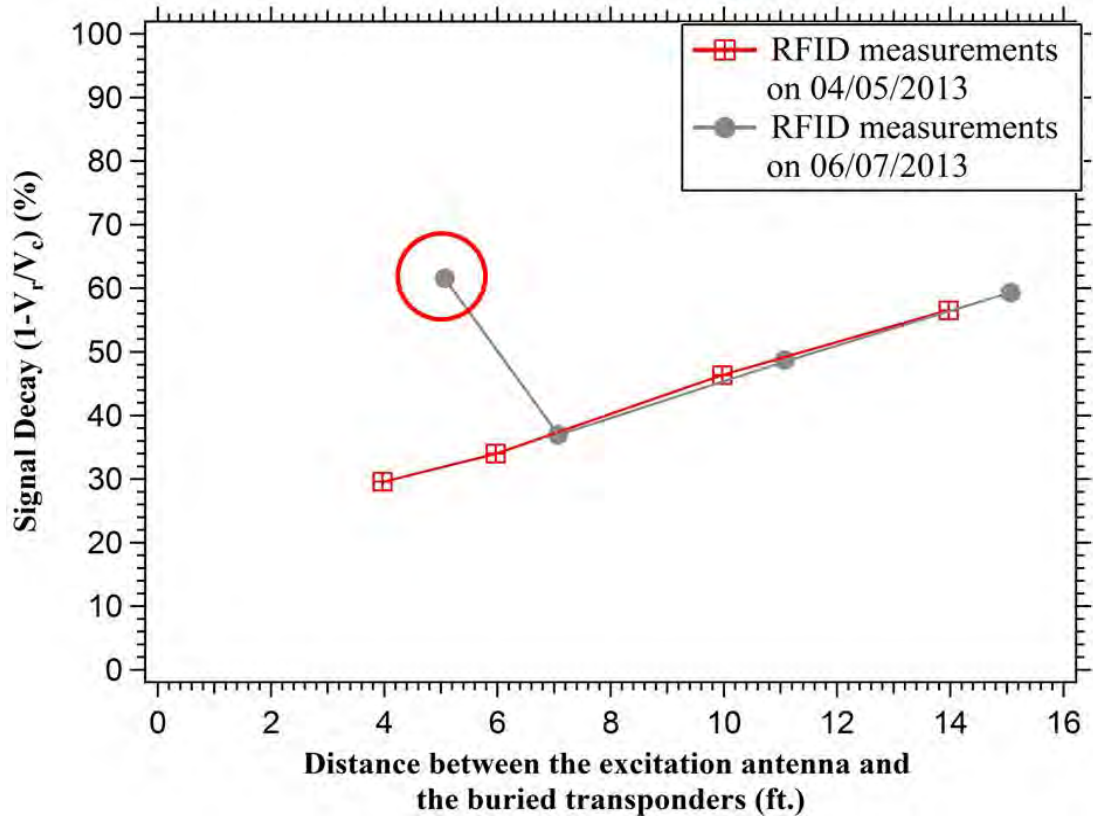


Figure 2-9. Transponder return RF signal strength decay curves in various mediums (i.e., air, water, sand and gravel) using the custom made excitation antenna developed by Papanicolaou research group.



3.

Figure 2-10. Processed RF signal strength decay curves corresponding to the two measurement dates during this reporting period: 04/05/2013 and 06/07/2013.

CONCLUSIONS AND SUMMARY

This research offers a new innovative approach for detecting scour in natural environments and/or around hydraulic structures. This innovation lies on the utilization of the Low Frequency (134.2 kHz), passive RFID technology to identify the onset of scour and provides a measure of scour depth. The main results of this study can be summarized as follows:

1. The material casing used to encapsulate the transponder plays a role to the system overall performance and should be taken into consideration at the designing phase of the project.
2. A key finding of this study is that the orientation of the transponder with respect to the excitation antenna plane plays a significant role in terms of the detection efficiency of the RF signal strength. A transponder that is placed perpendicular (favourable transponder orientation) to the excitation antenna plane provides the strongest signal and thus facilitates the largest detection distance. On the contrary, the transponder that is placed in parallel to the excitation antenna plane (unfavourable transponder orientation) limits the detection distance.
3. Another significant finding of this study is that medium matters. Transponders in sand, independent of the orientation of the excitation antenna, performed worse than transponders in air, water and gravel. Sand affects the RF signal strength due to the influence of the quartz particles to the electromagnetic field generated by the excitation antenna and the transponder inner antenna by deteriorating the RF signal propagation.
4. The findings from the analysis of the transponder return RF signal show that (i) the RF signal strength vs. distance decay curves are overall well represented by a linear fit; (ii) there is a shift between those line fits and a change in slope for different mediums. These findings led us to the following conclusions. First, if the RF signal decay curves are constructed reliably, then someone could extrapolate them to identify transponders' locations for larger distances, and secondly, for each set of application the user must know the dominant soil structure, since the soil medium affects the gradient of the RF signal strength decay curve.
5. The misplacement of the excitation antenna above the location of the transponder affects the RSSI value, leading to false conclusions about their actual distance. Therefore, the identification of the location of the buried transponders in the 3D domain using a triangulation scheme and the specifically developed RF signal strength curves for the soil type is a key feature of the RFID scour monitoring system.

4. OUTCOMES AND RECOMMENDATIONS

The need for maintenance personnel to be present at a bridge site could be removed by automating the collection and transmission of scour data, thereby making the scour-monitoring process safer and more efficient. An RFID system fitted with data telemetry equipment can provide the ability to collect and transmit data to a maintenance office. Remote monitoring could mitigate the inefficiencies and dangers inherent in the current practices, as well as provide early warning of impending bridge failure and the ability to track long-term degradation as a result of scouring. Additional benefits of remote monitoring include the potential reduction in the labor required to perform monitoring, and the acquisition of real-time data for calibrating scour prediction equations and enhancing the state of knowledge about the scour-monitoring process. *This evolving technology, once established, could offer new opportunities for field monitoring in large rivers (e.g., the Missouri River) and for understanding how sediment particles move or deposit around bridge structures (e.g., piers, abutments), spur dikes and weirs.* In addition, knowledge of the properties of the Lagrangian motion of individual particles via the RFID technology could provide rare datasets containing dynamic information regarding particle trajectories and displacement speeds near structures (e.g., Hunt and Papanicolaou, 2003; Papanicolaou et al., 2002).

These datasets could aid to the *fundamental understanding of clear water scour and live bed scour*. Clear water scour occurs when the amount of sediment transported from upstream of the scour hole is insufficient to fill the hole during the falling stage of the flood. Live bed scour occurs when sediments transported from upstream of a scour hole settle into the hole, sometimes completely refilling the hole, during the falling stage of the flood. *Live bed scour can be very difficult to detect by probing or visual inspection when the scour hole fills in after the process has occurred. Use of RFIDs could aid to the remote-monitoring of live bed scour.*

5. REFERENCES

- Allan, J.C., Roger H, Tranquili, J.V. "The use of Passive Integrated Transponder (PIT) Tags to Trace Cobble Transport in a Mixed Sand-and-Gravel Beach on the High-Energy Oregon Coast, USA." *Marine Geology* 232, (2006): 63-86.
- ASCE 2012. <http://content.asce.org/conferences/annual2012/>
- Barralet, M., X. Huang, and D. Sharma. "Effects of Antenna Polarization on RSSI Based Location Identification." *IEEE*, 2009.
- Chattaraj, A., S. Bansal, and A. Chandra. "An Intelligent Traffic Control System using RFID." *Potentials, IEEE* 28, no. 3 (2009): 40-43.
- Chen, G., D. Pommerenke, and R. Zheng. "Wireless Smart Rocks for Real Time Scour Monitoring." 2011.
- Choi, J. S., H. Lee, R. Elmasri, and D. W. Engels. "Localization Systems using Passive UHF RFID." *IEEE*, 2009.
- Chotiros, N. P. "Reply to `Biot Slow Waves in Sands Near the Seafloor, by R. D. Stoll " *J. Acoust. Soc. Am.* 103, (1998): 2726–2729.
- Clarke, R. H., Twede, D., Tazelaar, J. R. and Boyer, K. K. (2006), Radio frequency identification (RFID) performance: the effect of tag orientation and package contents. *Packag. Technol. Sci.*, 19: 45–54. doi: 10.1002/pts.714.
- Colorado State University, (1975). "Highways in the River Environment: Hydraulic and Environmental Design Considerations" prepared for the Federal Highway Administration, U.S. Department of Transportation, May 1975.
- Dittmer, K. "Blue Force Tracking: A Subset of Combat Identification." *Military Review* 84, no. 5 (2004): 38-40.
- Domdouzis, K., B. Kumar, and C. Anumba. "Radio-Frequency Identification (RFID) Applications: A Brief Introduction." *Advanced Engineering Informatics* 21, no. 4 (2007): 350-355.
- Dziadak, K., Sommerville, J., & Kumar, B. (2008). RFID based 3D buried assets location system.
- Dziadak, K., Kumar, B., & Sommerville, J. (2009). Model for the 3D location of buried assets based on RFID technology. *Journal of Computing in Civil Engineering*, 23(3), 148-159.

- Ettema, R., Nakato, T., and Muste, M. "An Illustrated Guide for Monitoring and Protecting Bridge Waterways Against Scour." *Iowa Highway Research Board Final Report, Project-515* (2006).
- Finkenzeller, K. *RFID Handbook: Fundamentals and Applications in Contactless Smart Cards, Radio Frequency Identification and Near-Field Communication* Wiley, 2010.
- Fukui, J. and Otuka, M. "Development of the New Inspection Method on Scour Condition Around Existing Bridge Foundations." *Proc., 1st Int. Conf. on Scour of Foundation, ICSF-1, Texas A&M Univ., College Station, Tex., 410–420.* (2002).
- Gaukler, G. M., R. W. Seifert, and W. H. Hausman. "Item-Level RFID in the Retail Supply Chain." *Production and Operations Management* 16, no. 1 (2007): 65-76.
- Goodrum, P. M., M. A. McLaren, and A. Durfee. "The Application of Active Radio Frequency Identification Technology for Tool Tracking on Construction Job Sites." *Automation in Construction* 15, no. 3 (2006): 292-302.
- Habersack, HM. "Radio-tracking Gravel Particles in a Large Braided River in New Zealand: A Field Test of the Stochastic Theory of Bed Load Transport Proposed by Einstein." *Hydrological Processes* 15, no. 3 (2001): 377-391.
- Hassan, T. and Chatterjee, S. "A Taxonomy for RFID." *Proceedings of the 39th Annual Hawaii International Conference on System Sciences, 2006. HICSS '06.* (2006).
- Hawrylak, P. J., M. H. Mickle, and K. McCane. *Remote Sensing for Bridge Scour* (2009).
- Jaselskis, E. J., M. R. Anderson, C. T. Jahren, Y. Rodriguez, and S. Njos. "Radio-Frequency Identification Applications in Construction Industry." *Journal of Construction Engineering and Management* 121, no. 2 (1995): 189-196.
- Jain, S. C , and Fischer, E. E. (1979). "Scour around bridge piers at high Froude numbers" Report No. FH-WA-RD-79-104, Federal Highway Administration, Washington, D.C.
- Joho, D., C. Plagemann, and W. Burgard. "Modeling RFID Signal Strength and Tag Detection for Localization and Mapping."IEEE, 2009.
- Khan, M. A. and V. K. Antiwal. "Location Estimation Technique using Extended 3-D LANDMARC Algorithm for Passive RFID Tag."IEEE, 2009.
- Ko, C. H. "RFID 3D Location Sensing Algorithms." *Automation in Construction* 19, (2010): 588-595.
- Kumar, B., & Sommerville, J. (2012). A model for RFID-based 3D location of buried assets. *Automation in Construction*, 21, 121-131.

- Lauth, T.J. and Papanicolaou, A.N. "Application of Radio Frequency Tracers to Individual and Group Particle Displacement within a Laboratory." *World Environmental and Water Resources Congress, 2009: Great Rivers* (2009).
- Liedermann, M., M. Tritthart, and H. Habersack. "Particle Path Characteristics at the Large gravel-bed River Danube: Results from a Tracer Study and Numerical Modelling." *Earth Surface Processes and Landforms* (2012).
- Li, N., & Becerik-Gerber, B. (2011). Performance-based evaluation of RFID-based indoor location sensing solutions for the built environment. *Advanced Engineering Informatics*, 25(3), 535-546.
- Nichols, M.H. "A Radio Frequency Identification System for Monitoring Coarse Sediment Particle Displacement." *Applied Engineering in Agriculture* 20, no. 6 (2004): 783-787.
- OREGON RFID. <http://www.oregonrfid.biz/>
- Papanicolaou, AN, M. Elhakeem, and A. Tsakiris. *Autonomous Measurements of Bridge Pier and Abutment Scour using Motion-Sensing Radio Transmitter* (2010).
- Papanicolaou, A.N., Moustakidis, I.V., Tsakiris, A.G. "Detection of Erosion Depth using a Passive RFID Technology." *River Flow*, September, 5-7, 2012. San Jose, Costa Rica.
- Rekik, Y., E. Sahin, and Y. Dallery. "Analysis of the Impact of the RFID Technology on Reducing Product Misplacement Errors at Retail Stores." *International Journal of Production Economics* 112, no. 1 (2008): 264-278.
- Roberts, C. M. "Radio Frequency Identification (RFID)." *Computers & Security* 25, no. 1 (2006): 18-26.
- Roussos, G. "Enabling RFID in Retail." *Computer* 39, no. 3 (2006): 25-30.
- Sellitto, C., S. Burgess, and P. Hawking. "Information Quality Attributes Associated with RFID-Derived Benefits in the Retail Supply Chain." *International Journal of Retail & Distribution Management* 35, no. 1 (2007): 69-87.
- Texas Instruments. "Antenna Reference Guide." *Literature Number SCBU025* (1996).
- Texas Instruments. "Low Frequency 23mm Glass Transponder." *Literature Number SCBS841* (2001).
- Texas Instruments. "Series 2000 Reader System Control Modules RI-CTL-MB2B RI-CTL-MB6B Reference Guide." *Literature Number SCBU044* (2008).

- Texas Instruments. "Series 2000 Reader System High Performance Remote Antenna-Reader Frequency Module RI-RFM-008B Antenna Tuning Board RI-ACC-008B Reference Guide." *Literature Number SCBU023* (2002).
- Wang, L. C., Y. C. Lin, and P. H. Lin. "Dynamic Mobile RFID-Based Supply Chain Control and Management System in Construction." *Advanced Engineering Informatics* 21, no. 4 (2007): 377-390.
- Wen, W. "A Dynamic and Automatic Traffic Light Control Expert System for Solving the Road Congestion Problem." *Expert Systems with Applications* 34, no. 4 (2008): 2370-2381.
- Wen, W. "An Intelligent Traffic Management Expert System with RFID Technology." *Expert Systems with Applications* 37, no. 4 (2010): 3024-3035.
- Zhao, J., Y. Zhang, and M. Ye. "Research on the Received Signal Strength Indication Location Algorithm for RFID System." IEEE, 2006.